



# Holocene coastal evolution and environmental changes in the lower Río Guadiaro valley, with particular focus on the Bronze to Iron Age harbour 'Montilla' of Los Castillejos de Alcorrín (Málaga, Andalusia, Spain)

Simon Matthias May<sup>1</sup>  | Helmut Brückner<sup>1</sup>  | Maike Norpoth<sup>1</sup> | Anna Pint<sup>1</sup> | Dennis Wolf<sup>1</sup> | Dominik Brill<sup>1</sup> | César León Martín<sup>2</sup> | Hans-Peter Stika<sup>3</sup> | José Suárez Padilla<sup>4</sup> | Pierre Moret<sup>5</sup> | Dirce Marzoli<sup>2</sup>

<sup>1</sup>Institute of Geography, Department of Geosciences, University of Cologne, Cologne, Germany

<sup>2</sup>Department of Madrid, German Archaeological Institute, Madrid, Spain

<sup>3</sup>Institute of Biology, Department of Molecular Botany, University of Hohenheim, Stuttgart, Germany

<sup>4</sup>Department of Historical Sciences, University of Malaga, Málaga, Spain

<sup>5</sup>Laboratoire TRACES—UMR 5608 du CNRS, Université de Toulouse, Toulouse, France

## Correspondence

Simon Matthias May, Institute of Geography, Department of Geosciences, University of Cologne, Cologne 50923, Germany.  
Email: [mays@uni-koeln.de](mailto:mays@uni-koeln.de)

## Funding information

Deutsche Forschungsgemeinschaft; Agence Nationale de la Recherche

## Abstract

Phoenicians were the first to systematically develop the area surrounding the Strait of Gibraltar at the end of the 9th century B.C. Following pioneering studies in the Río Guadiaro estuary (Málaga/Cádiz) in the 1980s, a German-Spanish cooperation project focussed on the role of indigenous people in the Phoenician colonisation trading networks at Los Castillejos de Alcorrín (Manilva, Málaga), one of the most important Early Iron Age settlements in southwestern Iberia. In the recent past, combined with systematic archaeological surveys, geoarchaeological research embedded in the interdisciplinary project 'Archeostraits' aimed at (i) deciphering palaeoenvironmental and coastal changes in the surroundings of Los Castillejos de Alcorrín throughout the mid- to late Holocene; (ii) constraining palaeoenvironmental conditions during early Phoenician colonisation; and (iii) better understanding human–environment interactions during the Final Bronze and Early Iron Age (i.e., end of 9th and 8th centuries B.C.). Coring transects along the Río Guadiaro allowed for differentiating successive palaeoenvironments and for establishing a chrono-stratigraphy for the Holocene sedimentary infill of the valley. Based on these results, the deposition of shallow marine sands, overlying deltaic deposits of alternating sand and mud, and the subsequent development of lagoonal conditions in the lower Guadiaro valley took place before the Phoenicians established the first settlements along the coast.

## KEYWORDS

connecting cultures, geoarchaeology, palaeoenvironmental evolution, Phoenician colonisation, Río Guadiaro, Strait of Gibraltar

Scientific editing by Christophe Morhange.

This is an open access article under the terms of the Creative Commons Attribution-NonCommercial-NoDerivs License, which permits use and distribution in any medium, provided the original work is properly cited, the use is non-commercial and no modifications or adaptations are made.

© 2022 The Authors. *Geoarchaeology* published by Wiley Periodicals LLC.

## 1 | INTRODUCTION

For a number of reasons, the narrow Strait of Gibraltar is an area of outstanding geological, prehistorical and historical significance and a place of far-reaching cultural contacts. Phoenicians were the first to systematically develop this area, which is of considerable geostrategic significance. Starting mainly from Tyros in today's Lebanon, they extended their colonial expansion across the Mediterranean beyond the Strait of Gibraltar at the end of the 9th century B.C. They laid the foundations of a pan-Mediterranean oikoumene (i.e., living space and settlement area of humans in the Mediterranean area) that included the coastlines of the southern Iberian Peninsula and northwestern Africa (Aubert, 2006, 2009, 2016; Marzoli, 2012, 2015, 2018, 2020; Pappa, 2013). The Strait of Gibraltar at the western end of the old world was thus transferred into a crucial point of different networks connecting three continents.

From an archaeological point of view, and particularly in the context of Phoenician research, the region has attracted remarkable attention since the 1980s: the studies of the Madrid Department of the German Archaeological Institute including coastal research in the Río Guadiaro estuary (Hoffmann, 1988a,b; Schubart, 1986, 1988) and the excavations of a Phoenician sanctuary in Gorham's Cave in the Rock of Gibraltar (Gutiérrez López et al., 2014) are prominent examples. The German-Spanish cooperation project at Los Castillejos de Alcorrín (Manilva, Málaga) focused on the role of the indigenous people in the Phoenician colonisation trading network (Marzoli, 2012; Marzoli et al., 2009, 2010, 2020a–d; Suárez Padilla & Marzoli, 2013). Excavations unearthed an indigenous settlement whose construction at the end of the 9th century B.C. was related to the Phoenician expansion. Its size, monumental fortification and peculiarity of the interior construction, structure and design are unique in the region and are among the earliest evidence of iron metallurgy in southwest Europe. The reasons for the abandonment of the site at the beginning of the 7th century B.C. are still unclear. Evidence of destruction is lacking. The findings rather point to an orderly abandonment that coincided with a restructuring of the indigenous settlement of the coastal regions of southern Spain and the expansion of the Phoenician port cities (Marzoli et al., 2020a,c).

Within the framework of the interdisciplinary research project 'Archeostraits' systematic archaeological surveys in the territory of Los Castillejos de Alcorrín produced new evidence of the territory's use from the Palaeolithic to the late Middle Ages (Marzoli, et al., 2020c); three settlements were discovered between Los Castillejos de Alcorrín and the Guadiaro river, with surface finds (i.e., handmade pottery of the local Late Bronze Age tradition and Western Phoenician wheelware) pointing to a close connection with Los Castillejos de Alcorrín. Apparently, the central site and the satellite settlements were founded and abandoned at the same time, likely documenting a centrally controlled settlement policy reacting to the Phoenician colonisation efforts on the part of powerful indigenous inhabitants (Marzoli et al., 2020a). The occupation of the territory was obviously connected to the Phoenician exploration of the strait, which from the end of the 9th century B.C. onwards led to the

emergence of new markets where the Phoenician maritime and indigenous continental economic areas met. The Guadiaro and favourable harbour locations near its mouth gained geopolitical importance (Marzoli, 2020; Marzoli et al., 2014).

The harbour settlement of Montilla, discovered in the course of the coastal research in 1987 (Hoffmann, 1988a,b), is only known fragmentarily. But based on the succession of pottery finds in three shallow excavations, it was possible to prove that it was an indigenous foundation that had close links with a Phoenician settlement probably located nearby (Schubart, 1988). Moreover, its connection with Los Castillejos de Alcorrín is evident. While the geoarchaeological research during the mid-1980s suggested a coastal embayment and direct marine access to Montilla (Hoffmann, 1988a,b; Schubart, 1988), these studies lacked detail, particularly in terms of the chronological resolution and the spatio-temporal evolution of palaeoenvironments in the surroundings of the site. In addition, as confirmed by a number of publications since then (e.g., Brisset et al., 2018; May et al., 2021; Vacchi et al., 2016), the decelerating rates of the relative sea-level (RSL) rise since 7000 B.P. facilitated a rather rapid lateral progradation of river deltas, the siltation of estuaries, and the evolution of floodplains, particularly in the lower stretches and estuaries of large rivers. These findings suggest that coastal evolution had already reached a rather mature state at the end of the mid-Holocene in many areas, challenging the previous interpretations of a direct marine access to Montilla and the timing of palaeoenvironments in general.

Therefore, within the framework of 'Archeostraits', geoarchaeological investigations were carried out in the estuary of the Río Guadiaro, one of the largest rivers in Mediterranean Andalusia (Figure 1). Based on detailed sedimentological, geochemical, chronological ( $^{14}\text{C}$ -AMS, OSL, diagnostic pottery) and microfaunal analyses of vibracores from the lower Río Guadiaro floodplain, the investigations aimed at (i) documenting the chronostratigraphy of the Guadiaro estuary along a number of coring transects; (ii) deciphering palaeoenvironmental and coastal changes in the Guadiaro estuary throughout the mid- to late Holocene; (iii) revealing palaeoenvironmental conditions and the accessibility of Montilla for ships during early Phoenician colonisation; and (iv) reconstructing the sea-level evolution for the study area and comparing it to other regional studies.

## 2 | PHYSICAL SETTING

### 2.1 | Geological, geomorphological and climatic setting

The study area is located in the active convergence zone between the African and Eurasian plates and belongs to the southwestern part of the Betic Cordillera, which stretches from the southeastern Iberian Peninsula to Morocco (Rif Cordilleras; Gibbons & Moreno, 2002; González-Castillo et al., 2015). The Betic Cordillera has evolved in the context of the Alpine orogeny from the Late Cretaceous onwards

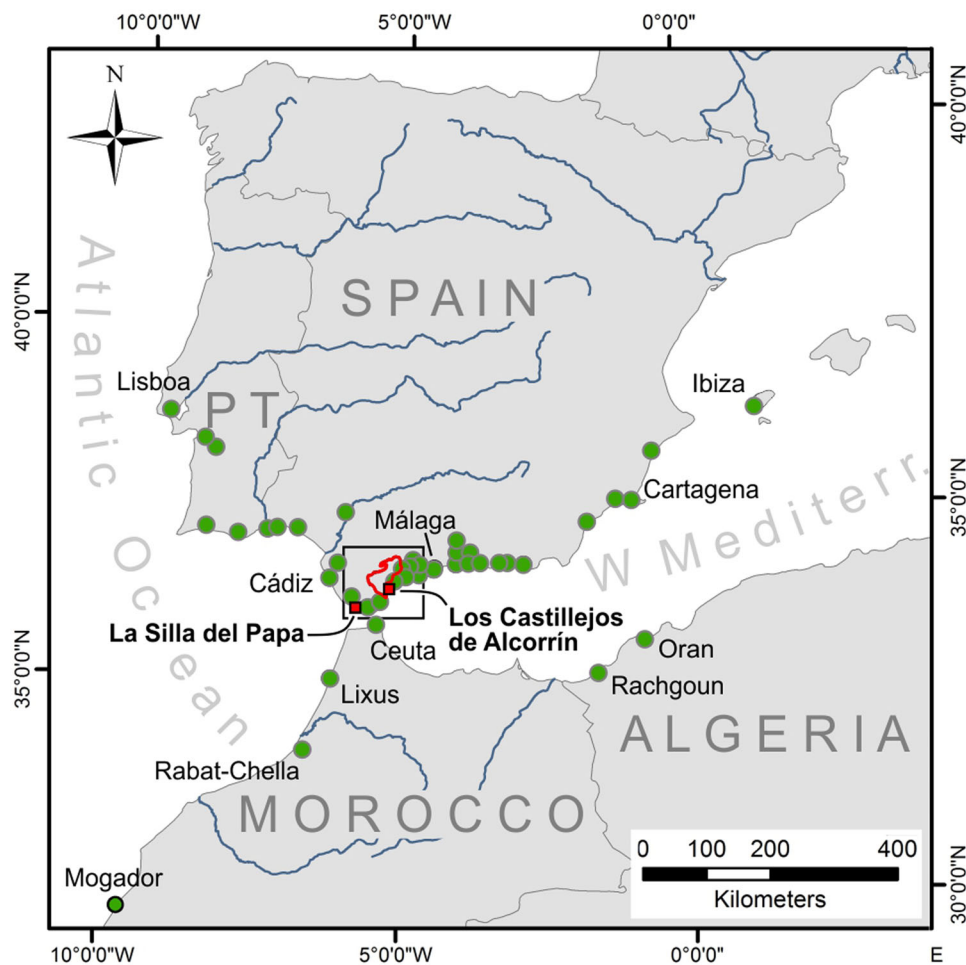


**FIGURE 1** Distribution of Phoenician settlements of the 8th and 7th centuries B.C. in the Western Mediterranean region and along the Atlantic coasts (green circles, compiled by D. Marzoli and E. Puch). The locations of La Silla del Papa and Los Castillejos de Alcorrín (red squares), both important Iron Age settlements of the southern Iberian Peninsula (e.g., Marzoli, 2012; Marzoli et al., 2010, 2020a,c; Moret et al., 2008, 2017) and in the focus of the Archeostraits project, as well as the Río Guadiaro catchment (red polygon) are depicted as well. [Color figure can be viewed at [wileyonlinelibrary.com](http://wileyonlinelibrary.com)]

(Gibbons & Moreno, 2002; Grützner et al., 2012; Vergés & Fernández, 2012).

The study area belongs to the Flysch zone, which comprises a series of isolated tectonic units between the internal and external zones of the Betic Cordillera as well as an extensive area west of Estepona (Martín-Chivelet et al., 2002; Reicherter & Peters, 2005). As part of this Gibraltar Flysch Zone (Reicherter & Peters, 2005), the lower reaches of the Río Guadiaro are surrounded by Paleogene to Neogene sand-, clay-, marl- and limestones (Aljibe and Algeciras Formations), which are partly covered by diverse post-orogenic Neogene to Quaternary deposits (e.g., alluvial and colluvial sediments, dunes), particularly in river valleys, local topographic depressions and coastal lowlands.

Displacements of the MIS 5e and 5c marine terraces suggest negligible rates of tectonic uplift or subsidence in the study area during the Late Quaternary (Zazo et al., 1999, 2008). In contrast, coastal uplift is highest at the Strait of Gibraltar (between Algeciras and Tarifa), some 30–40 km to the SW (Zazo et al., 1999). As

subsidence is inferred for the Mediterranean coastal areas east of Estepona (Zazo et al., 1999), the study area is situated in a transitional zone with elevations of ~6 and <2 m above the present mean sea level (asl) for the 5e and 5c terraces, respectively.

In the study area, the typical subtropical-Mediterranean Csa (Köppen & Geiger, 1968) climate with dry, hot summers and rather humid, mild winters (annual mean temp. ~18°C, annual mean precipitation 700 mm, mainly winter rain; Gutierrez de Ravae Aguera et al., 1986) is related to large fluctuations in water discharge of the majority of streams. Smaller arroyos are indicated by torrential runoff, while the larger perennial rivers (such as the Río Guadiaro) mostly originate in the higher parts of the Betic Cordillera and show considerable seasonal differences in discharge volumes and sediment transport. The average tidal range amounts to ~2 m in the Gulf of Cádiz and decreases to <40 cm along the adjacent Mediterranean coast, that is, in the study area. Superficial Atlantic waters enter the Mediterranean through the Strait of Gibraltar as fast-moving currents with seasonal fluctuations, resulting in anticyclonic eddies and a

seasonal rise in the summer mean sea level, and influencing coastal processes and oceanographic conditions in the Alborán Sea (Zazo et al., 1994).

## 2.2 | Holocene sea-level evolution and palaeoenvironments in southern Iberia

Following the last glacial maximum (LGM), rapid eustatically induced RSL rise with ~8 mm/year in the Western Mediterranean is inferred until 7500 B.P., when RSL reached ~7 m below the present mean sea level (bsl) (Lambeck et al., 2002; Vacchi et al., 2016). At that time, the maximum marine transgression is inferred at numerous places, for example the Gulf of Valencia at ~2 km inland of the present coastline (Brisset et al., 2018), and Mediterranean deltas such as the Ebro delta (Cearreta et al., 2016) developed due to rates of fluvial sediment input exceeding those of the decelerated RSL rise (0.6 mm/year). This period is also referred to as the highstand system track (HST; cf. Brisset et al., 2018) and was related to the progradation of prodeltaic deposits of the Spanish continental shelf (e.g., Río Guadalhorce; Fernández-Salas et al., 2003) or of beach-ridge systems such as documented from the gulfs of Almería and Valencia (Brisset et al., 2018; Goy et al., 2003). Further deceleration of RSL rise is inferred since 4000 B.P. (Vacchi et al., 2016); particularly during this period, glacial isostatic adjustment or active (neo)tectonics, paired with temporarily high sediment supply from the hinterland (Anthony et al., 2014), is considered the main driver for coastal changes, resulting in the continued progradation of coastlines.

Palaeoenvironmental changes in southern Spain are documented by changing vegetation patterns or fluctuating soil erosion, as typical for the entire Mediterranean. Landscape degradation is generally related to the successive aridification towards the semiarid conditions during the mid-Holocene (Jalut et al., 2009; Petit-Maire, 1990) and the human impact on vegetation and soil cover by deforestation and agriculture (Jalut et al., 2009). Most of these changes occurred contemporary to the presence of humans, and ambiguities remain about whether the key controls for the changing palaeoenvironments were the climate, human impact, or a combination of both (Bellin et al., 2013; Roberts et al., 2004; Roberts, 1990; Van Andel & Zangger, 1990; Wainwright, 1994; Wolf & Faust, 2015).

In SE Spain, the opening of the landscape may have started after c. 4400 B.P. (~2400 B.C.) during the late Chalcolithic. Successively increasing dryness, likely combined with intensified burning, pas-toralism, and forest destruction (Carrión et al., 2010) resulted in a change towards sclerophyllous vegetation. Anthropogenic influence (and disturbance) such as agriculture, mining, deforestation, and pastoralism is assumed to have peaked during and after the Roman occupation (approx. 1st century B.C.–3rd century A.D.). In addition, human-induced landscape degradation and desertification in SE Spain (Río Aguas) between 6000 and 500 B.P., that is, between the Late Neolithic and Medieval times, is inferred by Castro et al. (1998). Comparable findings are also documented from Cádiz Bay (Lagoon of El Gallo, SW Spain) (Arteaga et al., 2004, 2008; López Sáez

et al., 2002). Recent investigations on Lake Medina, situated some 80 km to the NE of the study area, brought evidence of an arid and warm climate during the early Holocene, which was followed by more humid conditions with high lake levels during the Holocene Climatic Optimum (7800–5500 B.P.) (Schröder et al., 2018). Since then, a progressive aridification (cf. Schirmacher et al., 2020) and the establishment of typical Mediterranean-type vegetation took place, whereas increasing anthropogenic impact was detected only during the last ~2000 years. Further studies on varved lake sediments in Zoñar Lake, Andalusia, suggest more humid conditions during the Roman Classical period (Iberian-Roman humid period, ~2600–1600 B.P.) and drier conditions from 2000 B.P. onwards (Martín-Puertas et al., 2009). This agrees with other studies reporting more humid conditions in the Mediterranean area at that time (Luterbacher et al., 2006; Roberts et al., 2004; Zanchetta et al., 2007). In the Lake Medina record, however, increased xerophilous and anthropogenic nitrophilous taxa indicate drier, warmer conditions and elevated human influence at that time (Schröder et al., 2018), which is in agreement with other marine and lake records (Corella et al., 2011; Moreno et al., 2012).

## 2.3 | Previous archaeological and geoarchaeological findings

Following preliminary research in 1985, archaeological excavations were carried out in the lower Guadiaro estuary at Montilla in 1986, just north of the modern highway A7, along the main road to San Enrique de Guadiaro (Figure 2). The excavations were restricted to three ~2–5 m long trenches east (slope; T1 and T2; Figure 2) and west (floodplain, at the foot of the slope; T3; Figures 2 and 12) of the main road, of which T2 and T3 are of major interest for this study. In T2 (Figure 12), that is, in the lower slope section, the archaeological strata directly cover the sandy Neogene bedrock and include basal cultural layers with settlement structures such as in-situ stone pavements, pits and fire places, covered by sediments and a palaeosol with abundant ceramic remains. Particularly based on this trench, Schubart (1986, 1988) concluded that Montilla was more and more influenced by the Phoenicians during the 8th century B.C., which is expressed in successively increasing proportions of wheel-thrown early Phoenician pottery in the archaeological strata. Similarities in pottery findings also point to a close relationship between Los Castillejos de Alcorrín to Montilla. In T3, that is, in the easternmost part of the floodplain, Neogene sandstone builds the base of the sedimentary succession as well, followed by a unit of grey loam with abundant ceramic remains at ~0.5–1.0 m asl. Then follows a 40–50-cm-thick, light brown sand layer, with several stones and an amphora handle at its upper boundary, which may have been intentionally put in place (Schubart, 1988). Above, a grey-brown loamy unit with abundant ceramic remains and stones was found. In this trench, West Phoenician wheel-thrown pottery dominates throughout the entire profile.

The archaeological findings raised questions about (i) the presence of an indigenous, Late Bronze Age and pre-Phoenician settlement site at

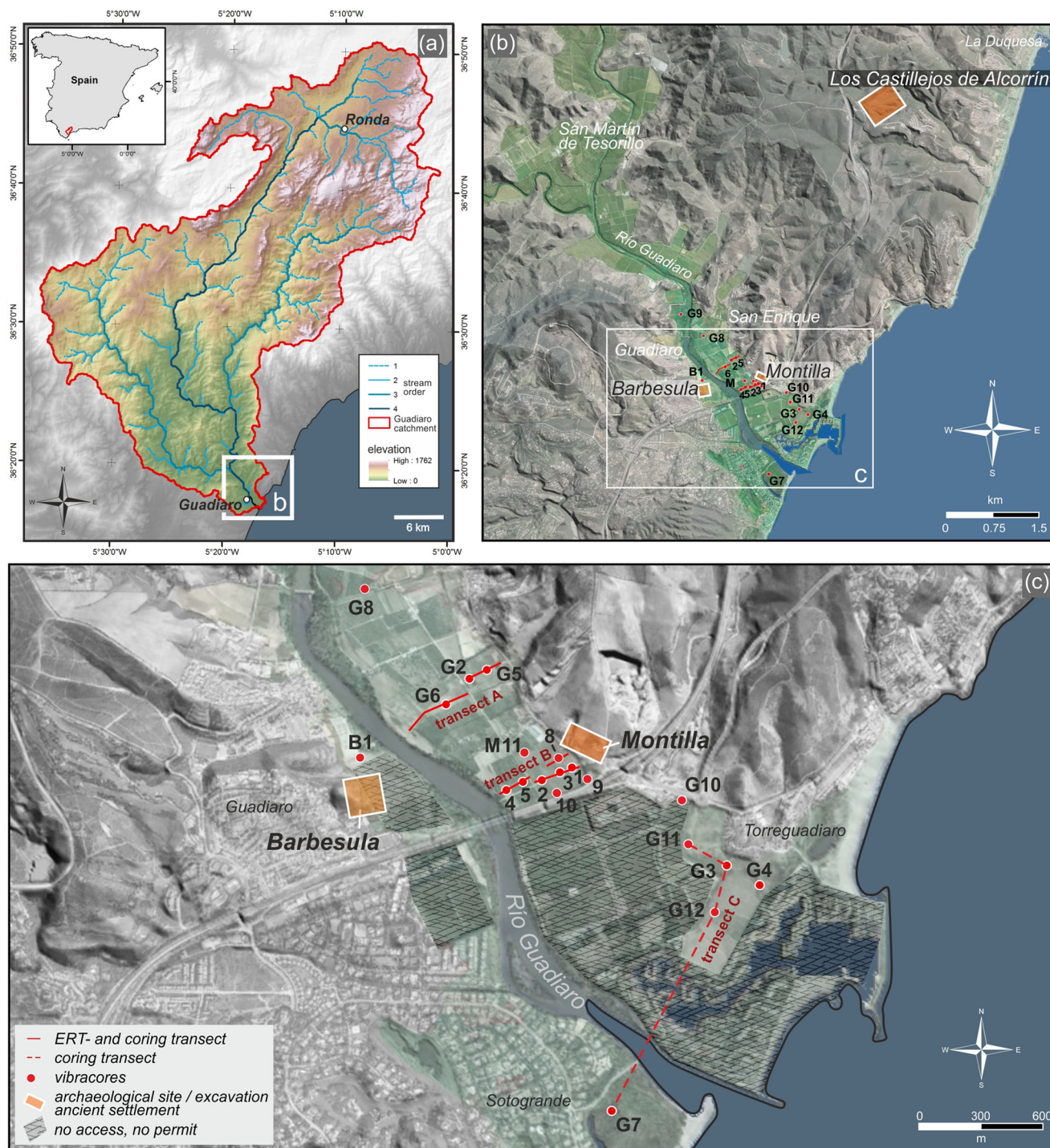


**FIGURE 2** Overview of the study area. (a) Location and catchment (red line) of the Río Guadiaro in the southern Iberian Peninsula, with stream orders 1–4. The study area is located in the southernmost and seaward part of the river catchment (image based on NASA SRTM data). (b) Lower Guadiaro floodplain and estuary between the river mouth and San Martín de Tesorillo together with coring locations. Los Castillejos de Alcorrín is located some 5.4 km northeast of the Río Guadiaro floodplain. (c) Detail of the Río Guadiaro estuary with coring locations and ERT transects; note that G9 lies outside of this area, northwest of G8. Locations of the Bronze Age to Iron Age I settlement Montilla and Iron Age II to Roman settlement Barbesula are indicated. Satellite image/elevation data in (a) and (b) based on Google Earth/Maxar Technologies (2011) and freely available LiDAR data of 2 m resolution (Geoportal of the Junta de Andalucía). ERT, electrical resistivity tomography. [Color figure can be viewed at [wileyonlinelibrary.com](https://onlinelibrary.wiley.com)]

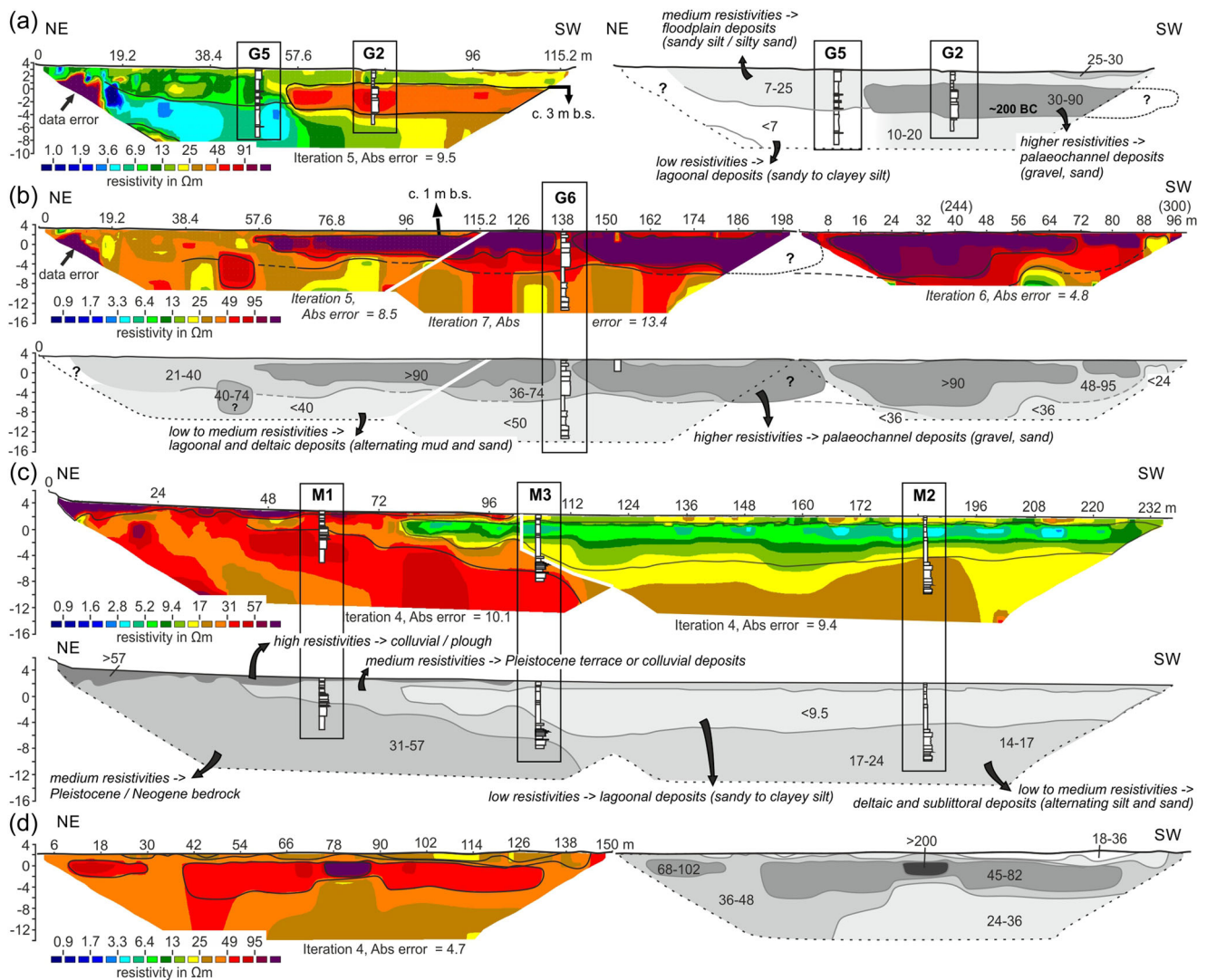


**FIGURE 3** ERT and coring transects A (a, b) and B (c, d). In general, the highest resistivities are related to coarse-grained channel deposits of the palaeo-Guadiaro (Facies E), as particularly found along transect A but also in the SW part of transect B (d). The lagoonal deposits (Facies C), found, for example, in M2 and M3, at the base of G5, and below the channel deposits in G2 and G6, are indicated by the lowest resistivities. Floodplain deposits (Facies F), the artefact-bearing layers in M1 (Facies O) and the shallow marine to deltaic sediments (Facies B) show low to medium resistivities. As indicated by the low resistivities along the NE section of transect B (c) above the pre-Holocene basement, no river channel deposits were found close to Montilla. ERT, electrical resistivity tomography. [Color figure can be viewed at [wileyonlinelibrary.com](http://wileyonlinelibrary.com)]

Montilla; (ii) the coastal configuration and palaeoenvironmental conditions in the Guadiaro estuary during the time of Phoenician contact; and (iii) the accessibility of Montilla by boat. Follow-up geoarchaeological research comprised coring transects in the direct vicinity of the excavations. Hoffmann (1988a) found that the boundary to the Neogene basement seems to slope towards the centre of the floodplain in the area of T3: in his core 39, located a few metres to the SW of T3 (Figure 12), a grey mud-dominated unit reaches down to 1.50 m bsl (5.70 m below surface [b.s.]), directly covering the Neogene basement. This layer was interpreted to be of marginal marine origin (Hoffmann, 1988a,b), related to a brackish environment; remains of wheel-thrown Phoenician pottery are reported to have been found in this unit as well. Hoffmann (1988a,b) thus assumed that (i) the coastline was located in direct adjacency to Montilla during Phoenician times, and moorage of

boats was possible in this area; (ii) trade of the Phoenicians with the local indigenous population was facilitated by a direct access to the site by boat. However, only very limited chronological information (i.e., lack of  $^{14}\text{C}$  ages) about the palaeoenvironmental conditions in the vicinity of the settlement and the palaeoenvironmental evolution in the lower Guadiaro valley in general was available.

### 3 | METHODS

#### 3.1 | Field work

Field work was carried out between 2015 and 2017, including geomorphological and geophysical surveys in the form of electrical

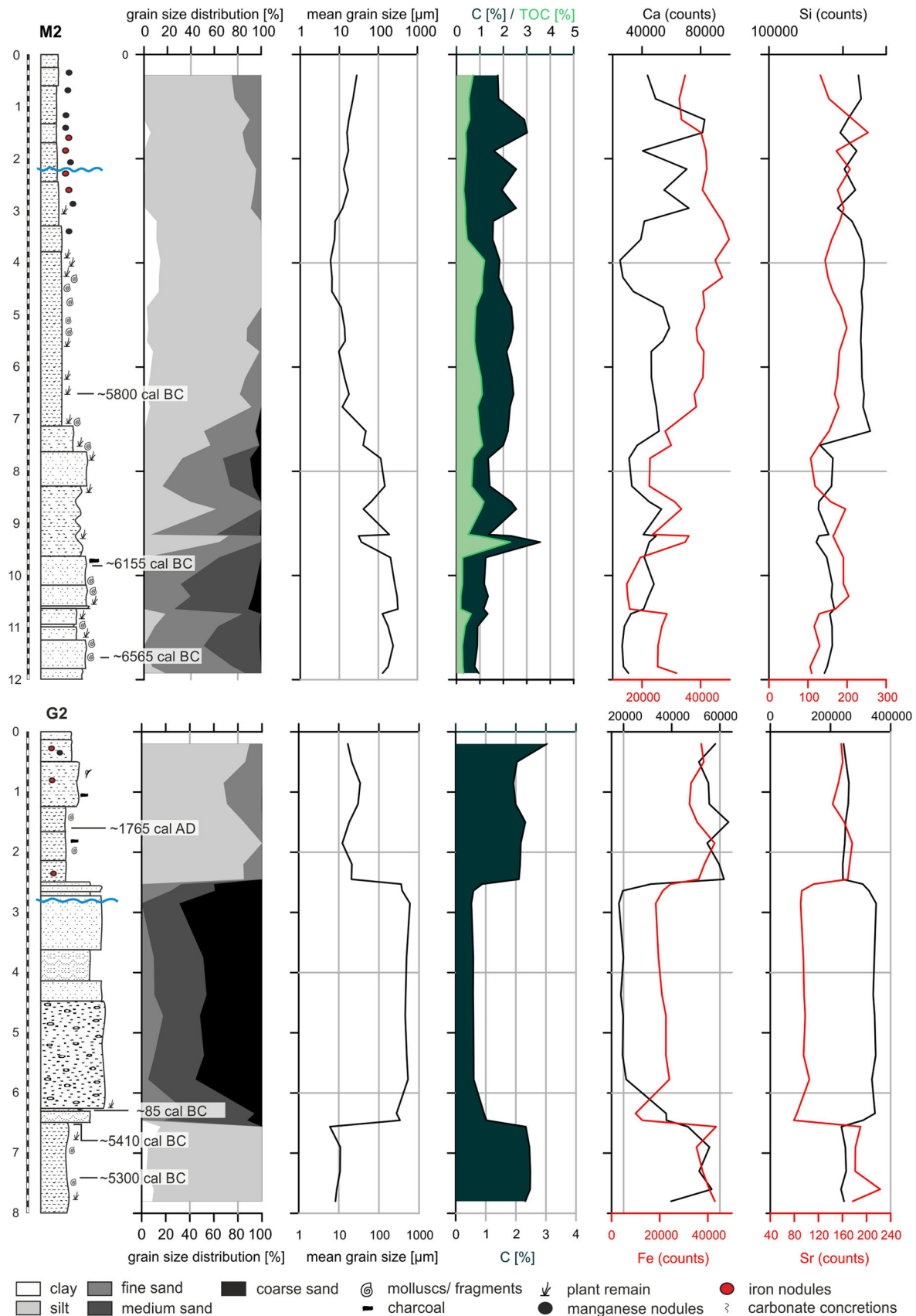


**FIGURE 4** Stratigraphy of cores M2 and G2, which contain the most important stratigraphical units described in this study. Granulometric (grain size distribution and mean grain size) and selected geochemical results (C or TOC, Ca, Fe, Si and Sr contents) as well as radiocarbon ages are shown as well. The blue wavy line represents the position of the present mean sea level. [Color figure can be viewed at [wileyonlinelibrary.com](https://onlinelibrary.wiley.com)]

resistivity tomography (ERT) measurements as well as the realisation of 22 vibracoring in the lower Guadiaro valley (Figure 2).

Geophysical surveys were performed along a total of 14 partly overlapping and valley-crossing ERT transects between February and September 2015 to detect subsurface sedimentary structures and characteristics of the sedimentary sequence and to extrapolate sediment facies determined in the sediment cores. The valley-crossing transects are combined with ERT transects A and B (Figures 2 and 3). The measurements were carried out with Wenner–Schlumberger electrode constellations using the GEO-LOG2000 multielectrode system (GeoTom, MK-RES/IP/SP) and electrode distances between 1 and 2 m. The software package RES2DINV (Geotomo Software) was used for processing the data.

The sediment cores (G2–G12, M1–M11) were drilled in the lower Guadiaro valley, between San Martín de Tesorillo and the Río Guadiaro estuary, with cores M1–M11 representing the direct vicinity of Montilla. A number of cores were arranged along the ERT transects A and B (Figures 2 and 3), which cross the valley floor in NE–SW direction. Transect C comprises the most seaward lying cores G3, 4, 7, and 10–12; no ERT measurements were carried out along this transect.

Coring was performed using an Atlas Copco Cobra vibracoring device with open steel auger heads of 5 and 6 cm outer diameters (G1–G12, M1–M5, M7, M9–M11, B1), and with closed steel auger heads containing 1 m long PVC tubes of 5 cm outer diameter (M6, M8). Open cores were documented in the field, and sediment samples were generally taken in 3–10 cm intervals, that is, in intervals representative of the stratigraphy. Closed cores M6 and M8 were used for high-resolution X-ray fluorescence (XRF) measurements (M6) and for OSL dating (M8). All coring sites were measured with a Topcon Hyper Pro DGPS (Differential GPS) with an accuracy of  $\leq 2$  cm for all three dimensions. Elevations asl and bsl are based on DGPS measurements of the back-barrier water level of the Río Guadiaro estuary, assumed to represent the mean tidal level.

## 3.2 | Lab work

### 3.2.1 | Sedimentological and geochemical analyses

Sedimentological and geochemical analyses (e.g., Figure 4) were carried out in the laboratories of the Institute of Geography, University of Cologne. For granulometric and geochemical analyses, the oven-dried (40°C) and hand-pestled sample material was sieved to separate fractions  $\leq 2$  mm (fine fraction) and  $> 2$  mm (coarse fraction). The fine fraction was taken for further analysis. For granulometric analyses, samples were pretreated with  $\text{H}_2\text{O}_2$  (30%) and 0.5 N  $\text{Na}_4\text{P}_2\text{O}_7$  (46 g/l) to remove organic carbon and for aggregate dispersion. The grain-size distribution of each sample was measured threefold using a Beckman Coulter LS 13320 Laser Particle Analyzer with 116-grain-size classes from 0.04 to 2000  $\mu\text{m}$ . Grain-size parameters were calculated using GRADISTAT software (Blott & Pye, 2001) and followed the nomenclature of Folk and Ward (1957).

For further analyses, the fine-grained fraction was ground using a planetary ball mill (Retsch MM 400). Total carbon (C) and nitrogen (N) contents were analysed by combusting the ground sample material ( $\sim 25$  mg) at 950°C using folded tin containers and a vario EL cube element analyzer (Elementar). For the determination of total organic carbon (TOC) contents, 20 mg of the sample material was filled in silver containers and measured after digesting with HCl (10%). The total inorganic content (TIC) was calculated by subtraction of TOC from C. The results were corrected by a daily factor based on the measurement of a known standard (Acetanilide).

Magnetic susceptibility (MS) was measured using an MS2E sensor and an MS3 MS metre (Bartington Instruments). XRF measurements on the compressed ground dry sample material ( $< 2$  mm) were performed with a portable XRF analytical instrument NITON XL3t 900 GOLDD (Thermo Fisher Scientific). XRF results refer to the average of three measurements and are given in counts.

Multivariate statistical analyses were applied for the samples of cores G2, G5–G9, G11, M1–M4, M7, and B1 (Figures 5 and 6) in the form of principal component analysis (PCA) for simplification of sedimentological and geochemical results and to determine sedimentary units and depositional facies using the PAST software (Hammer et al., 2001). Parameters were selected based on a prior inspection of the data set. Elements with data discontinuities as well as low concentrations and large errors were excluded, and Spearman's rank correlation coefficient was used to avoid autocorrelations. Variables TOC, Sr, Fe, Ca, Si, mean grain size, and sorting were used for PCA ( $n = 400$ ).

### 3.2.2 | Microfaunal investigations

For microfaunal analyses (e.g., Figure 7; Supporting Information: Figure S1), the 1 cm<sup>3</sup> fresh, non-dried sample material was wet-sieved using a 100  $\mu\text{m}$  mesh. Foraminifers and ostracods were handpicked under a stereoscopic microscope with a minimum of 300 tests per sample. Species identification was based on Armstrong and Brasier (2005), Cimerman and Langer (1991), Joachim and Langer (2008), Milker and Schmiel (2012), Pint et al. (2012) and the online database WoRMS (World Register of Marine Species) for foraminifers and ostracods. Classification into habitats was based on Murray (2006) for foraminifers and on Meisch (2000), Karanovic (2012) and Pint et al., (2012, 2015) for ostracods (Figure 7).

## 3.3 | Dating techniques

The chronological framework is based on altogether 36 <sup>14</sup>C-AMS ages, which were derived from samples of cores B, G and M. <sup>14</sup>C-AMS analysis was performed at the <sup>14</sup>CHRONO Centre for Climate, the Environment and Chronology, Queen's University Belfast (UK). Each sample was calibrated using the INTCAL20 or MARINE20 calibration datasets and Calib 8.2 software (Heaton et al., 2020; Reimer et al., 2020); <sup>14</sup>C-dated marine carbonates were corrected for



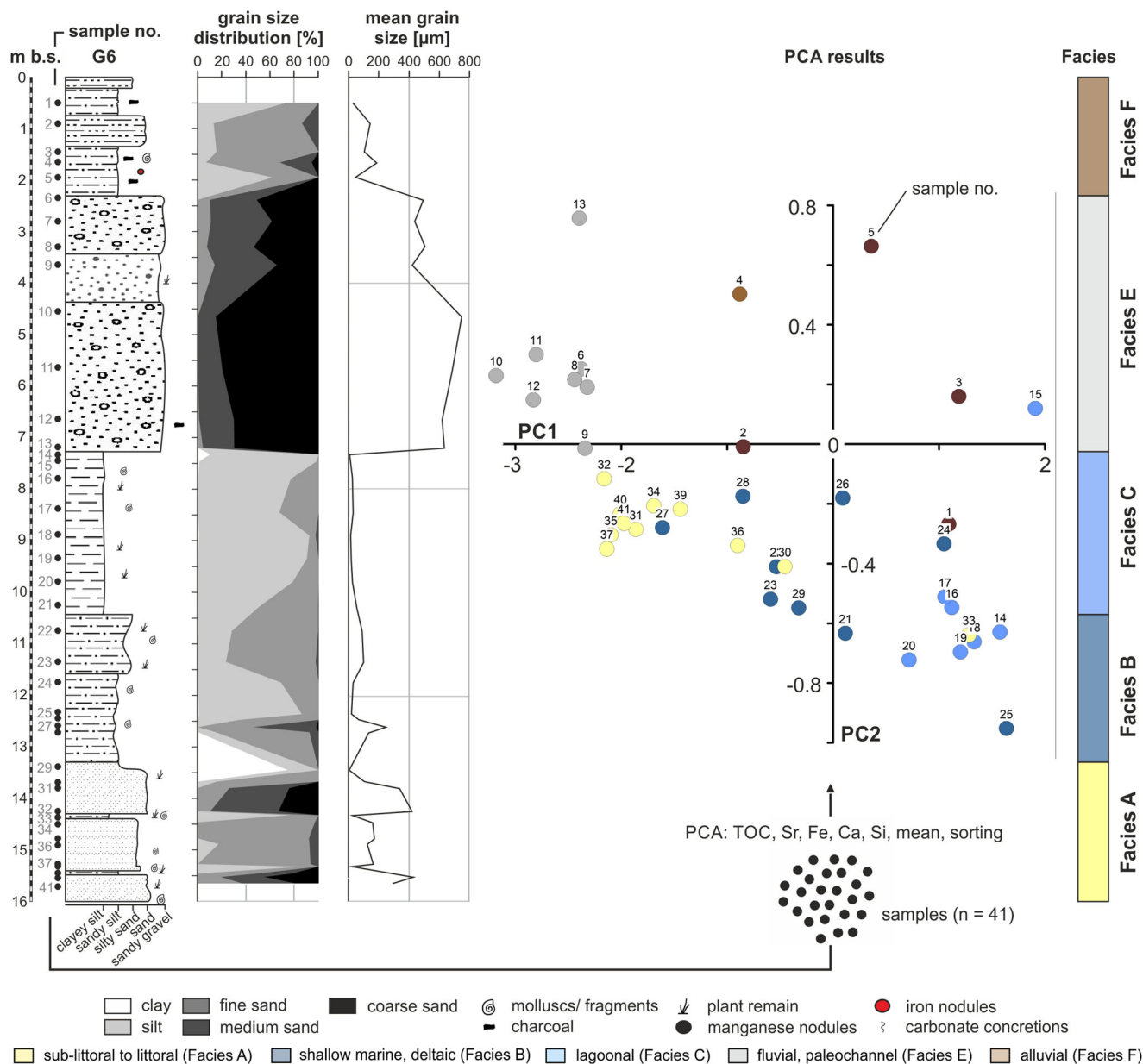


**FIGURE 5** Stratigraphy, sampling strategy (sample depth and sample numbers;  $n = 41$ ), distribution of sediment samples based on the PCA results (PCA based on TOC, Sr, Fe, Ca, Si, mean grain size, sorting), and, ultimately, classification into different facies, exemplified by sediment core G6. PCA results for all samples in this study ( $n = 400$ ) are shown in Figure 6. In general, samples from similar facies cluster based on their PCA values (i.e., based on the sedimentological and geochemical fingerprints). Facies A represents littoral to sublittoral; Facies B represents deltaic/fluviomarine; Facies C represents lagoonal; Facies D represents coastal lake/wetlands (freshwater-dominated); Facies E represents fluvial (channel deposits) and Facies F represents alluvial (overbank fines/floodplain). PCA, principal component analysis. [Color figure can be viewed at [wileyonlinelibrary.com](https://onlinelibrary.wiley.com)]

a local marine reservoir effect of  $\Delta R = -160 \pm 25$ , the weighted mean of 2 regional datapoints from the Marine Reservoir Correction Database (Heaton et al., 2020; Siani et al., 2000) (Table 1).

Two optically stimulated luminescence (OSL) samples were taken from closed core M6 (parallel core to M1; samples M6 OSL-1, M6 OSL-2) to verify/falsify a Holocene origin of the sterile sand sheet in M6 below the occupation layer/ground floor. Sample preparation and OSL measurements were performed under red-light conditions at the Cologne Luminescence Lab (CLL; Institute of Geography, University of Cologne). Analyses included dose rate estimation by means of

high-resolution gamma spectrometry, measurement of in-situ water contents, and calculation of cosmic dose rates following Prescott and Hutton (1994). Palaeodose determination was based on sand-sized (100–200  $\mu\text{m}$ ) quartz grains separated by a combination of dry sieving, HCl (10%) and  $\text{H}_2\text{O}_2$  (10%) treatment, density separation ( $2.62 \text{ g/cm}^3 < \text{quartz} < 2.68 \text{ g/cm}^3$ ) and HF etching (40% for 40 min). Small aliquots (1 mm) per sample were measured on a Risø TL/OSL reader equipped with blue LEDs and a U340 filter following the SAR protocol (Murray & Wintle, 2003). Protocol performance was evaluated with preheat plateau tests (preheat plateau between

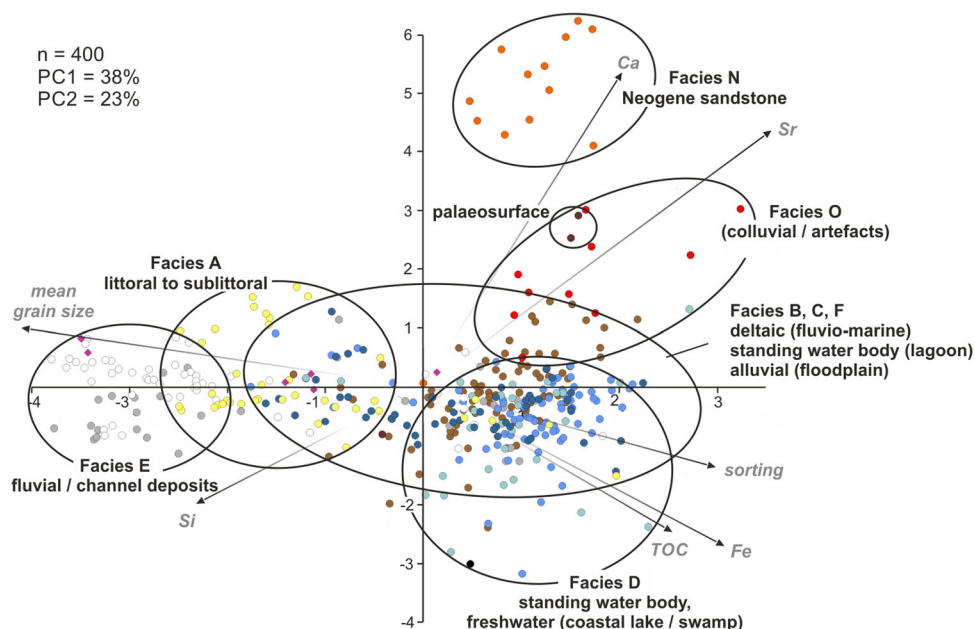


**FIGURE 6** PCA results of all samples taken from the sediment cores ( $n = 400$ ). PC1 and PC2 of the PCA together explain 61% of the variation. Distinct and mostly separate clusters are built by the littoral to sublittoral samples of Facies B, the channel deposits of Facies E and the samples from the Neogene basement (Facies N). Difficulties exist with the separation of fine-grained samples of facies C, D and F, which result from rather similar sedimentological and geochemical characteristics. However, samples from the alluvial Facies F show only slightly negative or positive values in PC2, whereas lagoonal Facies C and lacustrine Facies D are indicated by negative PC2 values in most cases. Facies B (delta-type samples) plots similar to Facies C and Facies A, as this facies is indicated by fluctuating depositional conditions, with an alternating influx of clastic sediment into a standing water body. The explanation for facies A–F, see Figures 3, 5, 9 and 12 and/or respective captions; Facies N represents Neogene sandstone and Facies O represents strata with anthropogenic remains. PCA, principal component analysis. [Color figure can be viewed at [wileyonlinelibrary.com](http://wileyonlinelibrary.com)]

180°C and 260°C) and dose recovery tests (dose recovery ratios of  $1.02 \pm 0.07$  for both samples). Palaeodoses (mean of 6–8 aliquots) were based on the central age model (CAM; Galbraith et al., 1999). Dose rates and luminescence ages were calculated with the DRAC software (Durcan et al., 2015).

Finally, archaeological remains comprised ceramic sherds/pottery taken from various sediment cores, for example, M1, M7 and B1 (Figure 8). The age of the pottery was estimated based on typology, composition and other characteristics.

## 4 | RESULTS AND FACIES INTERPRETATION

### 4.1 | Interpretation of artefact-bearing sediment units

In the upper core sections of B1 and M1, 3, 7 and 9, sediments contain abundant artefacts, mainly ceramic fragments. While these sediments give evidence of the human presence in the surroundings of the respective core sites during their deposition, they may not be defined as actual cultural layers or occupation horizons, that is, in the form of predominantly anthropogenic layers consisting of in-situ archaeological structures and/or deposits of clearly anthropogenic origin, at least

based on the findings presented here. The punctual information related to the 5–6 cm thick cores does not allow for evaluating the (lateral) stratigraphical context of the artefacts and the detection of in-situ structures such as anthropogenic pits, fire places, building remains or stone pavements, for which trenches/excavations would be required. Most of these units may rather relate to natural sediments containing artefacts, which are presumably reworked, not in-situ, and possibly washed down from hillslopes as colluvial sediments. In the upper part of core M7 (and presumably in cores M1 and 9 as well), however, a distinct layer of white to light brown silty sand with abundant sandstone and ceramic fragments was found at c. 1.20–1.40 m b.s., inside a ~2-m-thick loamy ceramic-bearing layer. At a comparable depth, Schubart (1988) described a similar layer with stones and an amphora handle at its upper boundary, for which an intentional settling/construction may be assumed. In addition, an indigenous cultural layer/occupation horizon of the Late Bronze Age with pits and fire places was inferred from T2, just a few tens of metres upslope of T3. Against this background, the stone-rich layer in cores M7, M1 and M9 suggests the presence of an anthropogenic cultural layer or occupation horizon at that depth in the easternmost floodplain sections of transect C, at least in the surroundings of M7. In this study, both the (colluvial) artefact-bearing natural sediments and the assumed occupation horizon (i.e., the stone layer) in M7 are summarised in Facies O.

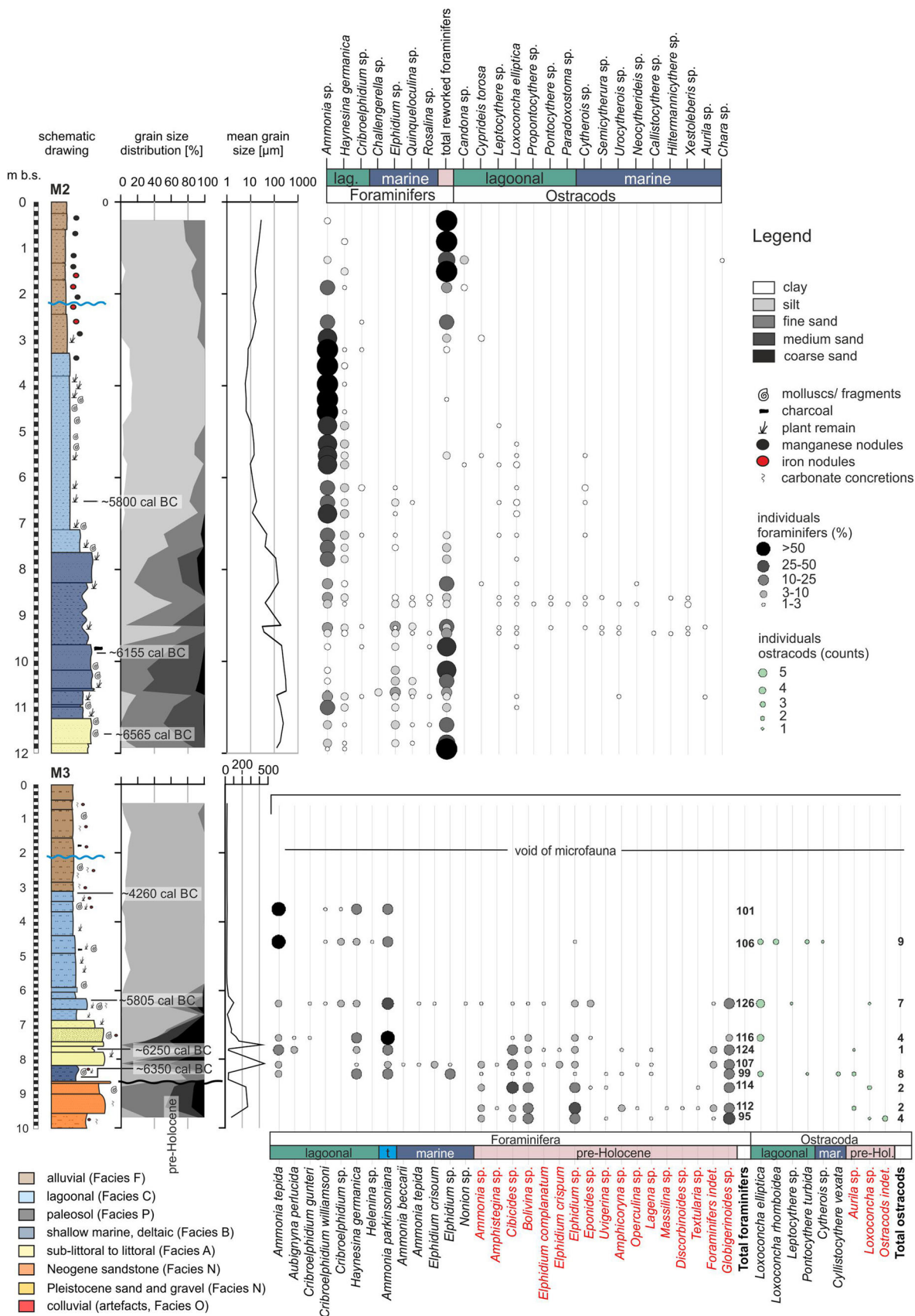


**FIGURE 7** Results of the micropalaeontological studies (Foraminifera, Ostracoda) and grain size data for cores M2 and M3. <sup>14</sup>C-AMS dating results (cf. Table 1) are shown as well. t represents marginal marine to lagoonal species. [Color figure can be viewed at [wileyonlinelibrary.com](http://wileyonlinelibrary.com)]

TABLE 1 <sup>14</sup>C-AMS dating results of all samples mentioned in this study

Transect	Core elevation (m asl)	Sample code	Depth (m b.s.)	Lab. code	Dated material	<sup>14</sup> C age (B.P.)	1σ max-min (cal B.C./A.D.)	2σ max-min (cal B.C./A.D.)
No transect	3.10	G8/12 PR	5.20	UBA35537	Leaf (remains)	4095 ± 48	2850–2573 B.C.	2872–2493 B.C.
	3.10	G8/20+ PR	7.64	UBA35538	Leaf (remains)	4081 ± 33	2838–2503 B.C.	2859–2492 B.C.
	3.10	G8/29 PR	13.40	UBA35539	<i>Rosmarinus</i> , <i>Pinus</i> (leaf)	7274 ± 44	6218–6073 B.C.	6230–6034 B.C.
	3.50	G9/13+ PR	7.53	UBA35540	Root (remains)	1895 ± 27	122–204 A.D.	75–220 A.D.
	3.50	G9/22 PR	10.73	UBA35541	<i>Pistacia</i> (leaf remains)	7225 ± 44	6213–6020 B.C.	6221–6011 B.C.
Transect A	2.85	G2/5 HK	1.59	UBA29226	Charcoal	198 ± 28	1660–1950 A.D.	1647–1950 A.D.
	2.85	G2/17 PR	6.28	UBA29228	Unid. PR	2071 ± 30	149–1 B.C.	169 B.C.–7 A.D.
	2.85	G2/20 PR		UBA31182	Unid. PR	6439 ± 52	5473–5373 B.C.	5481–5309 B.C.
	2.85	G2/22 PR	7.40	UBA29230	Unid. PR	6329 ± 38	5357–5220 B.C.	5373–5215 B.C.
	2.62	G6/12+ HR	7.13	UBA31239	Unid. PR or charcoal	3488 ± 62	1889–1698 B.C.	2007–1625 B.C.
	2.62	G6/19+ PR	9.57	UBA31240	Wood	7177 ± 43	6070–6010 B.C.	6212–5923 B.C.
	2.62	G6/40+ PR	15.56	UBA31242	Grape pip	7530 ± 68	6456–6265 B.C.	6477–6234 B.C.
	2.60	B1/6+ HK	2.97	UBA35533	Unid. plant remains	1942 ± 57	11–201 A.D.	45 B.C.–220 A.D.
	2.60	B1/24 PR	9.48	UBA35535	Unid. plant remains	7115 ± 40	6026–5922 B.C.	6066–5906 B.C.
	2.60	B1/34 PR	14.75	UBA35536	Sprout	7544 ± 38	6446–6391 B.C.	6467–6262 B.C.
Transect B	2.76	M1/8 HK	2.23	UBA31177	Charcoal	2572 ± 38	805–595 B.C.	809–549 B.C.
	2.06	M2/19 PR	6.55	UBA31183	Unid. PR + HK	6925 ± 40	5838–5743 B.C.	5961–5723 B.C.
	2.06	M2/30+ PR	9.84	UBA31184	Wood	7289 ± 76	6223–6076 B.C.	6368–6010 B.C.
	2.06	M2/36+ PR	11.60	UBA31185	Unid. PR + HK	7744 ± 44	6638–6505 B.C.	6645–6475 B.C.
	2.40	M3/7+ PR	3.42	UBA31178	Wood	5391 ± 39	4329–4174 B.C.	4339–4059 B.C.
	2.40	M3/15+ PR	6.24	UBA31179	Rhizome fragments	6927 ± 42	5840–5742 B.C.	5965–5723 B.C.
	2.40	M3/25 PR	7.74	UBA31180	Wood	7380 ± 40	6366–6099 B.C.	6377–6087 B.C.
	2.40	M3/27+ PR	8.55	UBA31181	Leaf remains	7484 ± 40	6417–6262 B.C.	6426–6244 B.C.
	2.35	M4/8 HK	2.42	UBA31186	Charcoal	476 ± 55	1403–1469 A.D.	1321–1621 A.D.
	2.35	M4/21 PR	7.76	UBA31187	Charcoal	7991 ± 41	7042–6827 B.C.	7051–6701 B.C.
	2.35	M4/25 M	9.67	UBA31189	Bivale (articulated)	7417 ± 38	5985–5830 B.C. <sup>a</sup>	6050–5744 B.C. <sup>a</sup>
	2.35	M4/35+ PR	12.70	UBA31190	Leaf (remains)	7247 ± 62	6219–6031 B.C.	6232–6006 B.C.
	2.76	M7/8+ PR	3.37	UBA33451	Unid. PR, rhizome	4065 ± 30	2663–2496 B.C.	2845–2475 B.C.
	2.76	M7/11 PR	3.84	UBA33450	Unid. PR, rhizome	5567 ± 34	4444–4358 B.C.	4455–4344 B.C.
Transect C	1.50	G3/4 HK	1.40	UBA29222	Charcoal	291 ± 24	1524–1648 A.D.	1509–1658 A.D.
	1.50	G3/8 PR	2.40	UBA29223	Unid. PR	231 ± 25	1646–1950 A.D.	1637–1950 A.D.
	1.50	G3/15 PR	4.37	UBA29224	Unid. PR	221 ± 26	1647–1950 A.D.	1641–1950 A.D.
	1.50	G3/22 M	5.10	UBA29225	Oyster ( <i>Ostrea</i> sp.)	1004 ± 23	1315–1423 A.D. <sup>a</sup>	1265–1480 A.D. <sup>a</sup>

TABLE 1 (Continued)

Transect	Core elevation (m asl)	Sample code	Depth (m b.s.)	Lab. code	Dated material	<sup>14</sup> C age (B.P.)	1σ max–min (cal B.C./A.D.)	2σ max–min (cal B.C./A.D.)
	0.50	G7/11 PR	5.98	UBA31243	Unid. PR + rhizome	3545 ± 71	2011–1769 B.C.	2130–1688 B.C.
	0.50	G7/32 PR	9.95	UBA31244	Unid. PR	6674 ± 40	5633–5557 B.C.	5664–5484 B.C.
	1.40	G11/20+ PR	6.75	UBA35543	Leaf/organic remains	5502 ± 37	4439–4272 B.C.	4445–4260 B.C.

Note: All ages were calibrated using CALIB 8.2 software and the data sets of Reimer et al. (2020).

Abbreviations: asl, above mean present sea level; b.s., below surface; HK, charcoal; Lab. code, UBA: <sup>14</sup>CHRONO Centre, Queen's University Belfast (UK); Unid. PR, unidentified plant remains.

<sup>a</sup>Corrected for a marine reservoir effect of  $\Delta R = -160 \pm 25$ , the weighted mean of 2 datapoints from the Marine Reservoir Correction Database (Heaton et al., 2020; Siani et al., 2000).

## 4.2 | Stratigraphy, facies interpretation and chronological results along transect A

The northeastern part of ERT and coring transect A (Figure 2) is characterised by low resistivities (<7 Ωm) at the base, which gradually pass into sediments with higher resistivities (7–25 Ωm) at 5–6 m b.s. (Figure 3a). Further towards the southwest (i.e., towards the Guadiaro river), wedge-shaped areas of higher resistivities >30 Ωm (partly >90 Ωm) appear between ~7 and ~3 m b.s. (Figure 3a), ~1 and 5.50 m b.s. and ~1 and ~10 m b.s. (Figure 3b), which are surrounded by sediments with resistivities of generally <40 Ωm.

As illustrated by sediment cores G2, 5 and 6 (cf. Figures 4, 5 and 10), areas of low resistivities in the ERT transect are related to fine-grained, silt-dominated sediments. Characteristics of these sediments with low resistivities, however, seem to vary considerably. At the base of G6, silty sand to sandy silt with numerous macrofaunal remains comprises the lower part of the core (16–12 m b.s.; Figure 5). These sediments are summarised in Facies A, which is interpreted to have a shallow marine, sublittoral to littoral origin (cf. Supporting Information: Table S1). In G6, Facies A is replaced by alternating layers of clay, silt and fine sand (12–10 m b.s.), which points to a fluctuating input of sand-sized clastic materials, separated by periods of still-water conditions. These deposits are summarised in Facies B (Supporting Information: Table S1), which is interpreted to reflect deltaic deposition into a shallow marine environment.

Subsequently, Facies B is covered by a unit of well-sorted, homogeneous, grey clayey silt (10–5 m b.s.), which accumulated under reducing conditions. In the lower part of this section (below 7.5 m b.s.), plant and mollusc remains are abundant, and articulated bivalves (*Cerastoderma* sp.) in living position were found. Based on the microfaunal analysis of core M2, lagoonal to brackish conditions can be assumed for these core sections, with dominant species *Ammonia tepida* (both juvenile and adult) and *Haynesina germanica* (foraminifers) and some lagoonal ostracods such as *Loxocochocha elliptica* (Figure 7). These sediments are summarised in lagoonal Facies C (Supporting Information: Table S1), indicated by brackish still-water conditions with reduced wave activity and low current

strength. Facies C was found at comparable depths of cores G2 and G5.

A slightly different preservation state of microfaunal specimens and the microfaunal assemblage with only few and partly reworked *Ammonia* sp. is found in the upper part of this fine-grained section (~7.5–5 m b.s.) (Figure 7). While samples from Facies C cluster together with the samples from this section in the PCA due to their similar sedimentological and geochemical characteristics (Figure 6), the microfaunal findings in this section may reflect changing palaeoecological conditions, for example, a decrease in salinity (Facies D, Supporting Information: Table S1).

In contrast to these rather fine-grained core sections with low resistivities, coarse-grained deposits of well-stratified sand and gravel were found at depths where higher resistivities of 30–90 Ωm (Figure 3a) or even >90 Ωm (Figure 3b) were measured (ERT transect A). In cores G6 and G2, a sharp boundary separates Facies D from these coarse-grained deposits, which show rather high (though fluctuating) mean grain size values above 700 μm; the sand/mud ratio is 95:5, the sediments are generally poorly sorted, Si contents increase, whereas C contents decrease (Figures 4 and 5). These coarse-grained layer can be interpreted as palaeo-channel deposits of the Río Guadiaro (Facies E, Supporting Information: Table S1). In core G2, Facies E was documented between 7 and 3 m b.s., in core G6 between 5.50 and 1 m b.s. Since the base of Facies E is related to a distinct and abrupt boundary, fluvial erosion during the deposition of Facies E is assumed, related to shifting channel courses.

On top of Facies E (G2 and G6) and in the upper part of G5, slightly stratified brown and fine-grained layers with high amounts of silt and fine sand and elevated C values (Figure 6) were found. Mean grain size values are generally low (<50 μm), the sand/mud ratio is 20:80 and sediments are rather poorly sorted. Samples from this unit cluster in the PCA, although overlapping with deposits from facies C and D (Figure 6). However, no microfaunal remains were found, except for a few reworked foraminifers. These strata indicate the deposition of alluvial sediments (overbank fines) from the Río Guadiaro (0–3 m b.s.) (Facies F), reflecting conditions similar to the present ones, that is, the successive accumulation of alluvial deposits

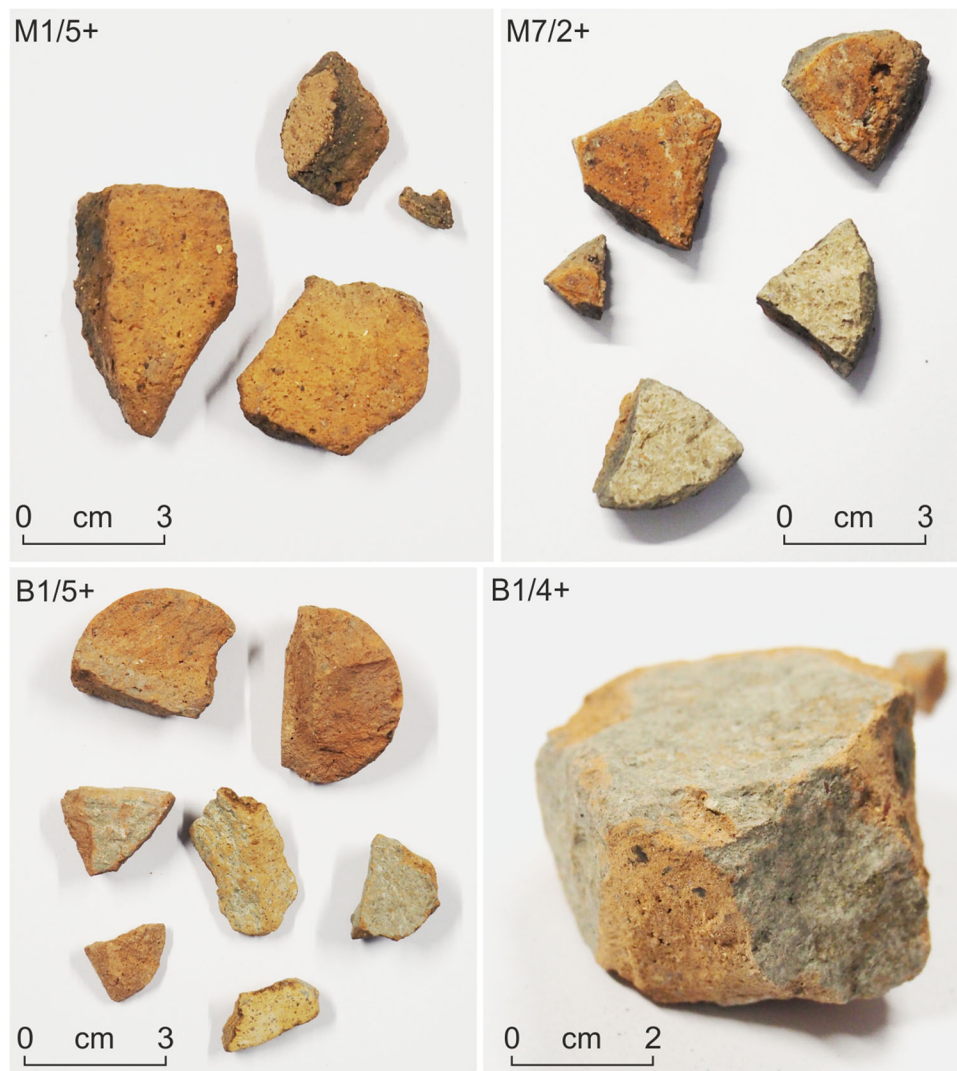


**FIGURE 8** Examples of pottery remains recovered from the sediment cores M1, M7 and B1. Ceramic fragments from M1 and M7 were classified as possibly Phoenician pottery, similar to the findings of Schubart (1988) (wheel-thrown pottery). Ceramic findings in core B1 date to Roman times. [Color figure can be viewed at [wileyonlinelibrary.com](https://onlinelibrary.wiley.com/terms-and-conditions)]

on top of the low-inclined floodplain of the lower Río Guadiaro (Supporting Information: Table S1). In G5, the transition from facies C/D to Facies F matches the transition of lowest (<7  $\Omega$ m) to moderate (7–25  $\Omega$ m) ERT values at ~7 m b.s. (Figure 3).

Finally, the westernmost core B1 slightly differs from the aforementioned cores and is generally indicated by quiescent depositional conditions in a marginal delta setting (Figures 9 and 11). The moderately sorted sand at the base of B1 possibly represents littoral deposits, which are followed by lagoonal mud with mollusks, some even in living position. The homogeneous lagoonal mud is covered by alternating layers of rather fine sandy to silty deposits. Except from the sand-dominated section between 7 and 8 m b.s., clear evidence of channel deposition, as documented for other cores from this transect (G2, G6), was not found in B1. However, in the upper part of the mud-dominated section (above 5 m b.s.), decreasing mollusc remains, and the light grey colour and signs of hydromorphy most likely mark the transition to freshwater conditions. Then, alluvial deposits (overbank

finer, Facies F) accumulated under subaerial exposure in the evolving floodplain. On top of this alluvium, a thick layer with abundant ceramic fragments (Facies O) was found above ~3 m b.s., in turn covered by another alluvial layer in the upper metre of the core.

Plant remains from the lower part of Facies E in G2 yielded an age of 169 cal B.C.–7 cal A.D. (G2/17 PR, Table 1), and plant remains from the underlying lagoon sequence were dated to 5481–5309 cal B.C. and 5373–5215 cal B.C., respectively (G2/20 PR at 6.40 m b.s. and G2/22+ PR at 7.40 m b.s., Table 1). Charcoal from Facies F yielded an age of 1647–1950 cal A.D. (1.59 m b.s., G2/5 HK).

At G6, a grape pip (*Vitis* sp.) taken from the prodeltaic deposits at 15.56 m b.s. resulted in an age of 6477–6234 cal B.C. (G6/40+ PR). Wood remains from the lagoonal deposits at 9.57 m b.s. were dated to 6212–5923 cal B.C. (G6/19+ PR). Plant remains from the lower part of Facies E were dated to 2007–1625 cal B.C. (G6/12+ HR, 7.13 m b.s.).

Finally, samples from core B1, located close to the Roman (or even Iron Age) settlement Barbesula and thus on the western bank of

the Río Guadiaro, resulted in  $^{14}\text{C}$ -ages of 6467–6262 cal B.C. (sprout, B1/34 PR, 14.75 m b.s., Facies A), 6066–5906 cal B.C. (B1/24 PR, 9.48 m b.s., Facies C) and 45 cal B.C.–220 cal A.D. (B1/6+ HK, 2.97 m b.s., Facies O). In the same ceramic-rich layer (3–1 m b.s.), numerous remains of Roman pottery were found, for which, however, a particular period could not be determined (Table 1).

### 4.3 | Stratigraphy, facies interpretation and chronological results in the landward part of the study area (cores G8 and G9)

G9 and G8 represent the northernmost cores in this study (Figures 9 and 10). Since the sediments show overall comparable characteristics to those in the seaward cores of transect A, we only briefly document the facies succession of cores G8 and G9 (cf. Supporting Information: Table S1). At G9, the sedimentary succession starts with deltaic Facies B, followed by lagoonal (Facies C) and then freshwater conditions (Facies D) (11.00 and 7.50 m b.s.). After an abrupt and likely erosive boundary, channel deposits of the Río Guadiaro (Facies E) were documented (7.50–2.50 m b.s.), covered by stratified overbank fines (Facies F). Likewise, Facies B builds the lowermost part of G8 until 7.30 m b.s. as well, similar to a number of cores of transects A and B (Figures 9–12). Here, these deltaic deposits are intercalated by Facies E (palaeo-channel of the Río Guadiaro)

between 11 and 8.00 m b.s. Above, Facies E represents a further shift of the Río Guadiaro to the position of G8 (7.30 and 6.20 m b.s.), followed by facies D (freshwater conditions) and the transition to subaerial conditions of Facies F (overbank fines, 4.90 m b.s. upwards).

At G9, the transition from deltaic deposits (Facies B) to the overlying lagoon (Facies C) was dated ~6100 cal. B.C. (G9/22 PR, 10.73 m). Directly below the thick unit of channel deposits in G9 (7.53 m b.s., G9/13+ PR), the root remains from the freshwater deposits were dated 75–220 cal. A.D., indicating that the Río Guadiaro channel shifted to this place sometime after A.D. ~75. In G8, remains of rosemary (*Rosmarinus* sp.) and pine (*Pinus* sp.) taken from the sand-dominated base at 13.40 m were dated ~6100 cal. B.C. (G8/29 PR). Between these two periods of channel deposition, plant remains were dated ~2600 cal B.C. (G8/20+ PR, 7.64 m). At 5.20 m, leaf remains date ~2600 cal B.C. (G8/12 PR) as well, taken from freshwater Facies D, just before the floodplain evolved (cf. Table 1).

### 4.4 | Stratigraphy, facies interpretation and chronological results along transect B

ERT and coring transect B (Figures 2 and 3c,d) stretch between the foot slope directly below the former excavation area of the Montilla archaeological site and the Guadiaro River. Comparable with the depositional sequence of G6, core M2 (Figures 4 and 7) starts with

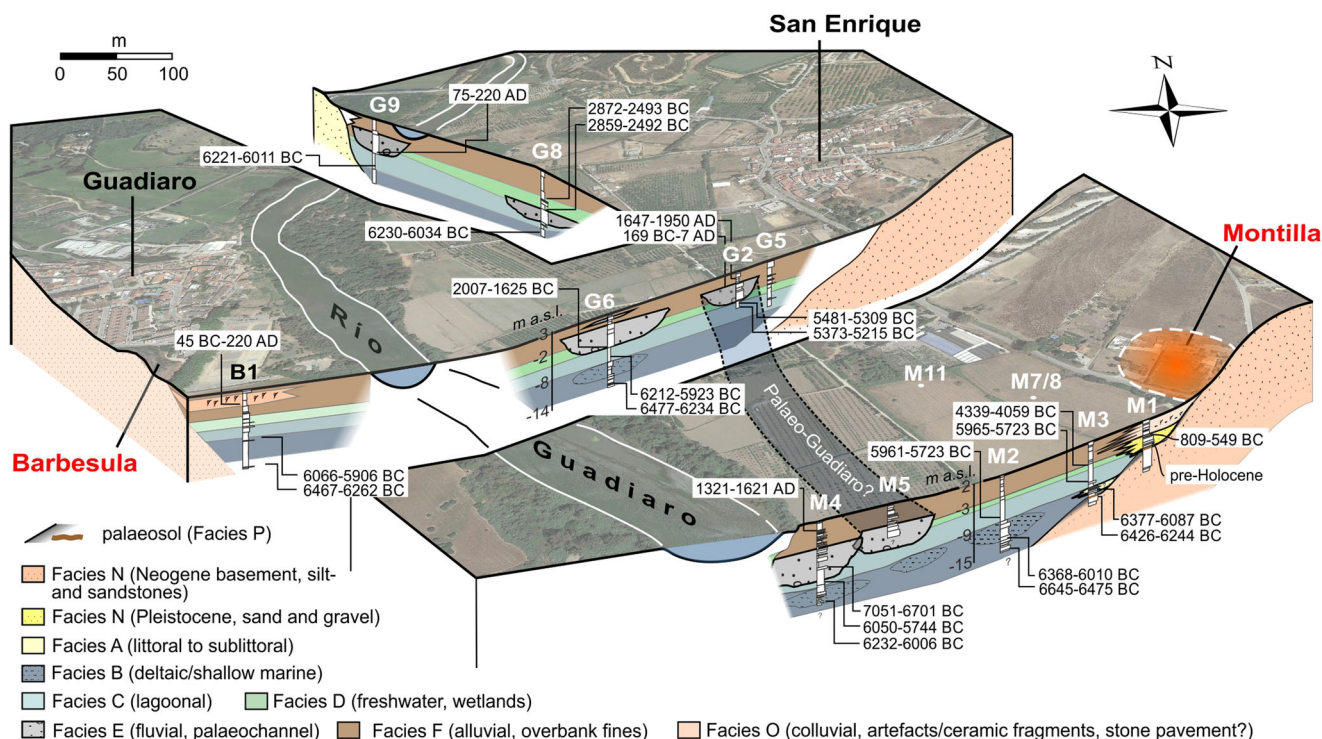


**FIGURE 9** Oblique view of the facies distribution along coring transects A and B, as well as between transect A and the most landward cores G8 and G9;  $^{14}\text{C}$ -AMS ages are depicted (all ages given in cal B.C./A.D.). As documented by G8, G2 and G6, palaeo-channels of the Río Guadiaro, dated between 1800 and ~85 cal B.C., were located closer to Montilla than the present channel. Direct river access to Montilla, however, could not be confirmed; no river channel deposits were found in the directly adjacent cores (background: satellite image from Google Earth/Maxar Technologies, 2011). [Color figure can be viewed at [wileyonlinelibrary.com](http://wileyonlinelibrary.com)]

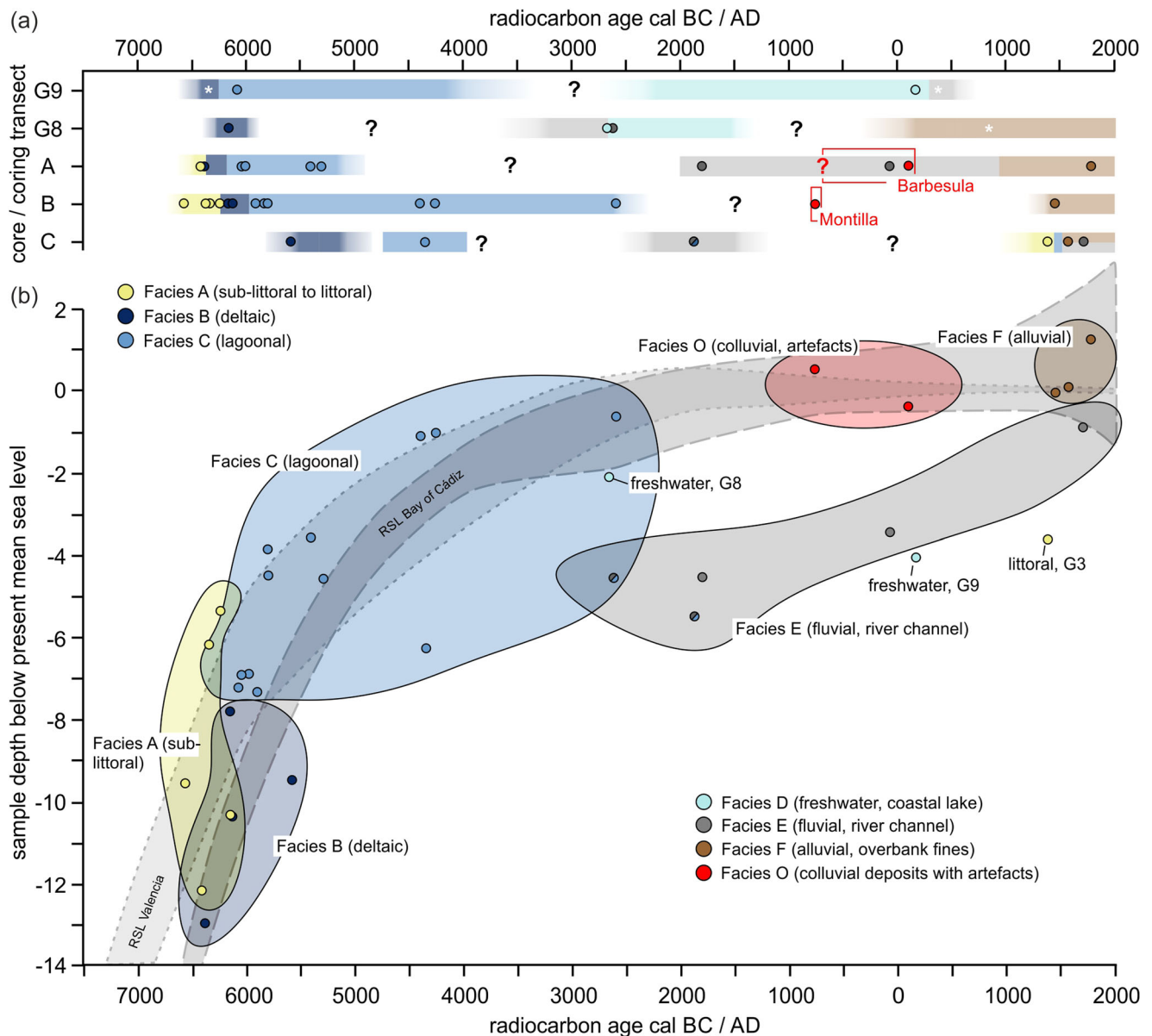


**FIGURE 10** (a) Chronological distribution of facies in the most landward cores G9 and G8, as well as along coring transects A–C. (b) Age-depth plot of facies defined in the study area. Both graphs illustrate the palaeoenvironmental changes in the study area since the end of the early Holocene. Interestingly, all littoral to deltaic deposits were dated before 5500 cal B.C., and lagoonal conditions were documented between approx. 6000 cal B.C. and 2500 cal B.C.; after this period, almost all  $^{14}\text{C}$ -AMS age estimates are from fluvial, anthropogenic and alluvial facies E and F, documenting that a river-dominated landscape had established in the study area already during the Bronze Age. Relative sea level (RSL) envelope curves from the Algarve region and the Bay of Cádiz (Atlantic; García-Artola et al., 2018; May et al., 2021) and Valencia (Vacchi et al., 2016) are depicted as well. Elevations of facies found in this study are in considerable agreement with RSL evolution in the Bay of Valencia. [Color figure can be viewed at [wileyonlinelibrary.com](http://wileyonlinelibrary.com)]

littoral deposits at the base (12.00–10.20 m b.s., Facies A), followed by the fluctuating conditions of deltaic Facies B (10.00–7.00 m b.s.) and Facies C (7.00–approx. 3.50 m b.s.) (Figure 7; Supporting Information: Table S1). The depth of the latter facies matches the low resistivities of  $<17\ \Omega\text{m}$  (mostly  $<9.5\ \Omega\text{m}$ ) documented in the uppermost 6 m of the ERT transect (Figure 3c) between ~75 m and 250 m transect length (Figure 3c). In the upper part of this mud-dominated sequence, the microfauna is almost entirely made up of *Ammonia* sp., reflecting decreasing salinity (Facies D). The alluvial

sediments of the Río Guadiaro (Facies E) follow above 3.00 m b.s., which correspond to slightly increased resistivities of c. 13–24  $\Omega\text{m}$  (Figure 3).

At M3, the weathered pre-Holocene (likely Neogene) basement occurs below 8.70 m b.s. Here, only reworked foraminifers were found (Figure 7), and sediments are indicated by medium to low resistivities of  $>30\ \Omega\text{m}$ . As suggested by the ERT transect and cores M2 and M3, the upper boundary of this Facies N (cf. Supporting Information: Table S1) declines towards the Río Guadiaro, reaching



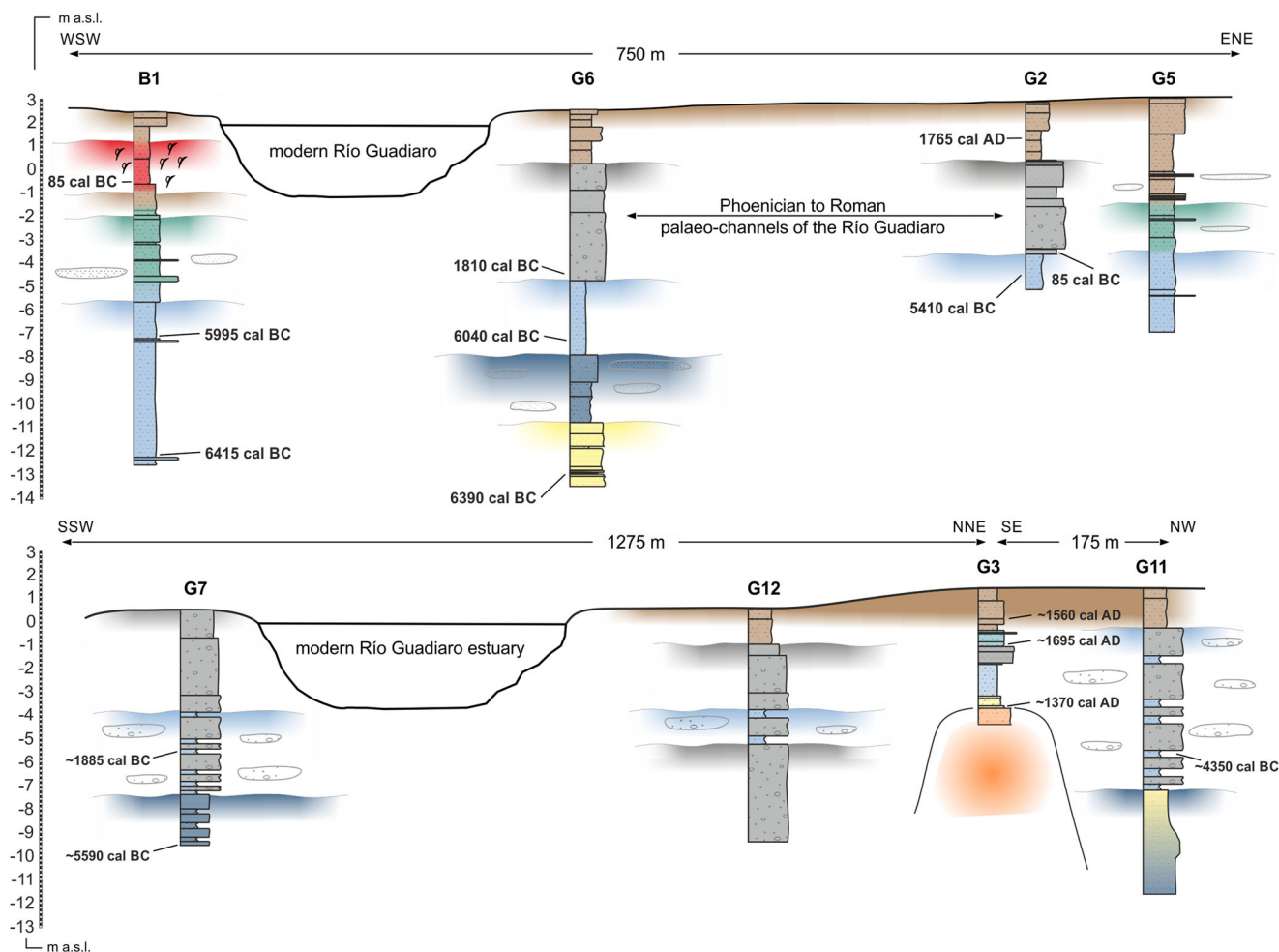


**FIGURE 11** Coring transects A and C with facies distribution and  $^{14}\text{C}$ -AMS age estimates. For facies explanation, see Figures 3, 5, 9 and 12 and/or respective captions. [Color figure can be viewed at [wileyonlinelibrary.com](http://wileyonlinelibrary.com)]

elevations below 10 m b.s. at ~120 m transect length, between M2 and M3. Above Facies N, however, the Holocene sedimentary sequence in M3 is comparable to the one described for M2, that is, reflecting the transition from Facies A (8.70–7.00 m b.s.) to Facies C (7–3 m b.s.) and then Facies F (above 3 m b.s.) (cf. Supporting Information: Table S1). While the typical facies succession (i.e., A, B, C, D) was found in M4 as well, channel sediments of a former course of the Río Guadiaro (Facies E) are present in M4 and M5, related to a wedge-type area of high resistivities of 45–82  $\Omega\text{m}$  between 2 and 6–7 m b.s. (Figure 3d). Interestingly, in the middle of this wedge, a ~10 m long and ~2 m thick section of >200  $\Omega\text{m}$  was found ~80 m from the Río Guadiaro at a similar depth, potentially pointing to an anthropogenic structure.

In the northeastern part of ERT transect B, cores M1 and M7–M9 were drilled at the foot slope directly below the former excavation area of the Montilla archaeological site (Figure 12). At the base of M1, the partly cemented and intensely weathered yellow sand is associated with resistivities of >30  $\Omega\text{m}$  and interpreted as the weathered sedimentary rock of Neogene age (cf. Hoffmann, 1988b) (Facies N), which was found at the base of M3 as well; its upper

boundary rises towards the NE (Figure 3c). Facies N is topped by a thin layer of gravel in a red, clayey matrix that can be interpreted as a palaeo-surface, analogous to previous investigations in the surroundings of Montilla (Hoffmann, 1988b) (Facies P). This palaeo-surface is covered by a sequence of sterile brown medium sand, which in turn is overlain by a thin, brown, clay- and silt-containing stratum at 2.20 m b.s. (Facies P). Above, brown to grey, poorly sorted and rather heterogeneous deposits were found, which are dominated by silt and fine sand, contain abundant ceramic fragments, and show even higher resistivities of >50  $\Omega\text{m}$  (uppermost 1–2 m, Figure 3c). Most of the pottery was classified as ceramics from indigenous production. These layers are interpreted as artefact-containing colluvial sediments, related to the nearby settlement of Montilla (Facies O; cf. Supporting Information: Table S1).

While a similar sedimentary sequence exists at M9, a slightly different sequence was found at M7/8, located a few decametres from T3 described in Hoffmann (1988b) and Schubart (1988) (Figure 12). Here, the weathered Neogene basement (Facies N) and the subsequent thin palaeo-surface (Facies P) (5.0–4.0 m b.s.) are covered by homogeneous, grey to grey-black clayey silt with

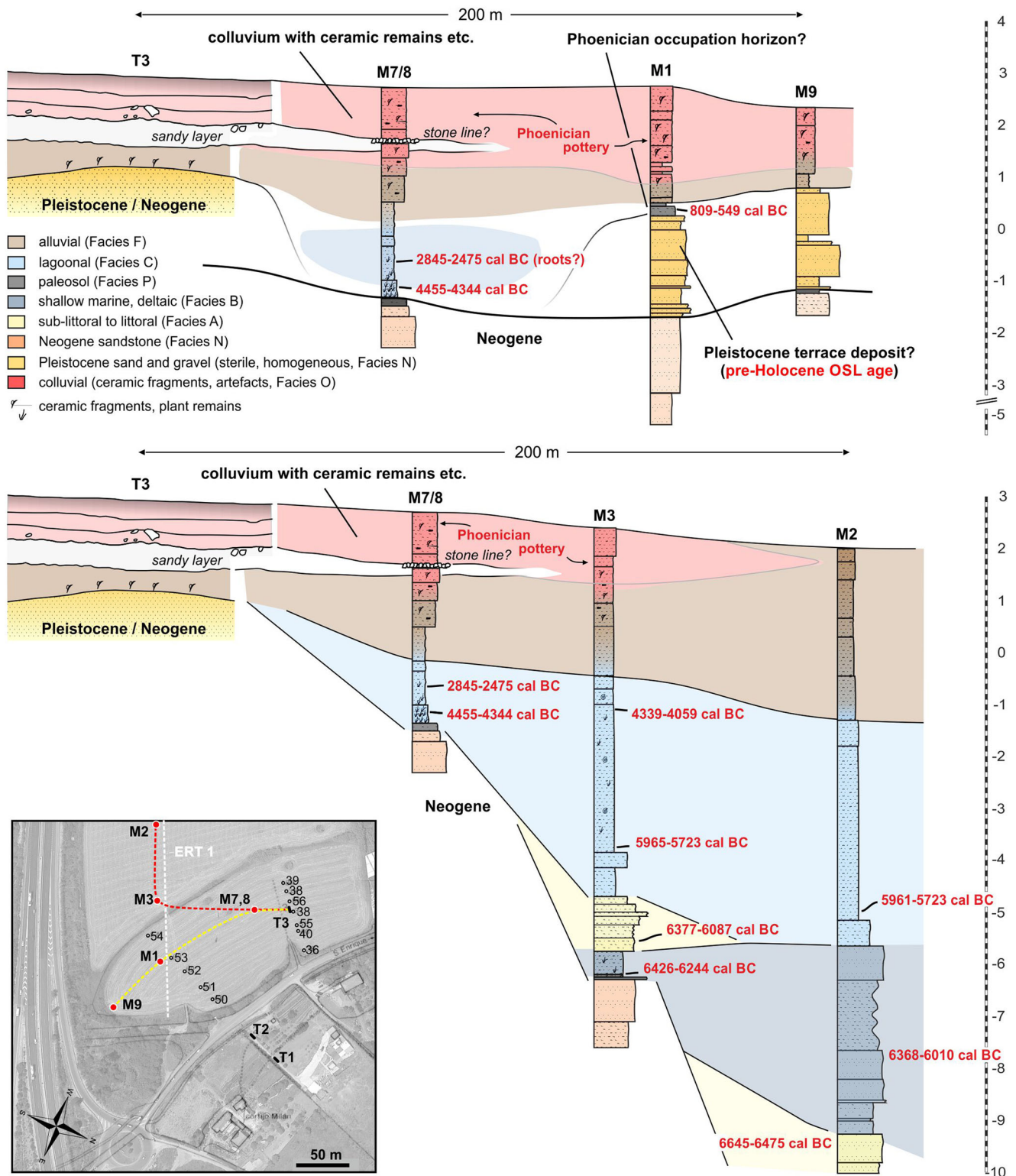


**FIGURE 12** Eastward section of coring transect B, that is, cores in the surroundings of Montilla, with facies distribution and <sup>14</sup>C-AMS age estimates. The map in the lower left (satellite image from Google Earth/Maxar Technologies, 2011) shows the location of cores carried out in this study (M1–3, 7–9) and in the study of Hoffmann (1988a,b; numbers 50–54 and 36–40, 55–56). T1–T3: archaeological excavations/trenches as described in Schubart (1988); profile T3 reproduced from Schubart (1988); the elevation of trench T3 was adjusted to the cores of this study due to apparent differences in measurements. [Color figure can be viewed at [wileyonlinelibrary.com](http://wileyonlinelibrary.com)]

abundant plant remains (4.0–3.0 m b.s.), interpreted to represent sediments related to Facies C. Above follows dark brown clayey silt with numerous signs of hydromorphic conditions (i.e., Fe and Mn spots), containing a few gastropod remains, several well-rounded gravels and small indeterminate ceramic fragments. These deposits resemble the alluvial strata found in the upper part of cores M2 and 3 (Facies E). However, between 2 and 0 m b.s., brown-grey, loamy and heterogeneous sediments with abundant charcoal remains and ceramic fragments occur (Facies O), similar to core M1. At ~1 m b.s., a distinct layer of white to light brown silty sand with abundant pieces of sandstone and ceramic fragments interdigitates with these deposits (Figure 12). Several attempts to retrieve further sediment cores in the surroundings of M7/8 had to be stopped at approximately this depth due to high resistance during drilling.

Altogether 13 <sup>14</sup>C-AMS ages are available for transect B. At M1, charcoal remains from the palaeosol and/or occupation layer or ground floor at 2.23 m b.s. (M1/8 HK) were dated to 809–549 cal B.C. The sterile sand below this occupation layer/ground floor was OSL-dated to a pre-Holocene age (>190 ka for M6 OSL-1, >230 ka for M6 OSL-2; minimum ages due to saturation of the quartz signal in both samples). Peat-like sediments, found directly on top of the Neogene basement at M7, were dated to 4455–4344 cal B.C. (M7/11 PR, 3.84 m b.s.). Above, plant remains (possibly root fragments) from 3.37 m b.s., that is lagoonal Facies C, date to 2845–2475 cal B.C. (M7/8+ PR). At M3, shallow marine deposits (Facies B, 8.55 m b.s., M3/27+ PR) were dated to 6426–6244 cal B.C. and plant remains from an organic layer above to 6377–6087 cal B.C. (M3/25 PR, 7.74 m b.s.). Subsequently, plant remains from the lower part of lagoonal Facies C (M3/15+ PR, 6.24 m b.s.) and the upper part of Facies D (or the lower part of Facies F; M3/7+ PR, 3.42 m b.s.) resulted in ages of 5965–5723 cal B.C. and 4339–4059 cal B.C., respectively. At M2, littoral deposits (Facies A) were dated to 6645–6475 cal B.C. (M2/36+ PR, 11.60 m b.s.) and deltaic deposits to 6368–6010 cal B.C. (M2/30+ PR, 9.84 m b.s.). Plant remains from the lower part of lagoonal Facies C are 5961–5723 cal B.C. (M2/19 PR, 6.55 m b.s.) <sup>14</sup>C-years old. Finally, samples from M4 resulted in ages of 6232–6006 cal B.C. (Facies B, M4/35+ PR, 12.70 m b.s.), 6050–5744 cal B.C. (Facies C, M4/25 M, 9.67 m b.s.), 7051–6701 cal B.C. (probably reworked, Facies E, M4/21 PR, 7.76 m b.s.) and 1321–1621 cal A.D. (M4/8 HK, 2.42 m b.s., Facies F) (Table 1).

#### 4.5 | Stratigraphy, facies interpretation and chronological results along transect C

In the seaward part of the lower Guadiaro Valley, just south of the village of Torreguadiaro and thus close to the northeastern margin of the floodplain, coring G3 of transect C (Figures 2 and 11) reveals sediments of Facies A (with *Ostrea* sp., 5.75–5.15 m b.s.) immediately on top of the base rock (Facies N). Subsequently, clearly laminated deposits dominated by silt and clay suggest rather quiescent depositional conditions with a fluctuating input of clastic materials and varying production of organic materials (Figure 11). These

deposits are covered by rather homogeneous grey fine sand between 2 and 2.40 m b.s. (Facies E) and, finally, topped by Facies F.

Sand-dominated deposits of facies A were found at G11 (Figures 2 and 11) between 13 and 7 m b.s. as well. Between 7 and 1.70 m b.s., fluctuating depositional conditions were likely related to shifting river channels of the lower Guadiaro (Facies E) into a lagoonal environment (Facies C). The last channel deposit at 2.20–1.70 m b.s. is covered by floodplain strata (Facies F).

At G7, comparable to G11, units of sandy gravel (Facies E) and interdigitated mud (Facies C) alternate between 8 and 5 m b.s. at G7, that is, in the area of the southwestern bank of the modern Río Guadiaro (Figures 2 and 11). This sequence is followed by a rather thick unit of sandy gravel (5–0 m b.s.), likely related to the evolution of the modern Río Guadiaro estuary channel. At the base of G7, quite well-sorted sand with interdigitated homogeneous grey mud is interpreted to be of sublittoral origin, just seaward of the estuary mouth (Facies B, deltaic deposits), where the alternating accumulation of sand and mud can be explained by a fluctuating input of clastic sediments.

The radiocarbon ages of core G3 (Figures 10 and 11) indicate that these floodplain sections silted up only recently. The basal oyster fragments were dated ~1350 cal A.D. (G3/22 M, Table 1). Above, unidentified plant remains show <sup>14</sup>C-ages of 1641–1950 cal A.D. (G3/15 PR, 4.37 m b.s.) and 1637–1950 cal A.D. (G3/8 PR, 2.40 m b.s.), while charcoal from 1.40 m b.s. was dated 1509–1658 cal A.D. (G3/4 HK). Lagoonal deposits at 6.75 m b.s. are 4445–4260 cal B.C. <sup>14</sup>C-years old (leaf remains, G11/20+ PR) some 250 m to the west of G3. Finally, on the southwestern bank of the modern Río Guadiaro, plant remains from 5.98 m (G7/11 PR, alternating facies C and E) and 9.95 m b.s. (G7/32 PR, Facies B) were dated to 2130–1688 cal B.C. and 5664–5484 cal B.C., respectively (Table 1).

## 5 | DISCUSSION

### 5.1 | Chronostratigraphical interpretation and palaeoenvironmental evolution in the lower Río Guadiaro in the context of human presence

Shallow marine to littoral sediments were most likely reached at the base of cores G6 (transect A) and M2 to M4 of transect B (Figures 9–12). Related to the high rates of eustatic sea-level rise until ~6000 B.C. (~8000 B.P.), as documented for numerous coastal areas worldwide and also in the western Mediterranean (Vacchi et al., 2016) until the end of the early Holocene (cf. Dabrio et al., 2000; Fernández-Salas et al., 2003; Zazo et al., 2008), delta-type sediments of shallow marine origin subsequently accumulated in the centre of the Guadiaro Valley covering the littoral sands of Facies A, as documented by cores M2 and 4 as well as in G6, G8 and G9. They are characterised by alternating sand and mud layers and were related to fluctuating depositional conditions, likely due to varying sediment inputs by the prograding Río Guadiaro mouth and/or adjacent littoral environments. The basal shallow marine to littoral and subsequent

delta-type deposits (facies A and B) are older than 6000 B.C., except for the basal layers of core G7 (Figures 10 and 11). Delta-type deposits were found at the base of the most landward core G9, giving evidence of a more landward position of the Río Guadiaro mouth before ~6000 B.C., that is, related to a landward shift of the coastline during the rapid eustatic sea-level rise until ~6000 B.C. (~8000 B.P.). This agrees with existing sea-level data from the area (Lario et al., 2002; Fernández-Salas et al., 2003; Zazo et al., 2008) and suggests that the shallow marine to littoral deposits below the delta-type facies date back to the transition from early to mid-Holocene (7th–6th millennium B.C.), that is, the end of the Epi-Palaeolithic period (before 6500 B.C.) (Figure 13a). However, no human occupation is documented in the directly adjacent area at that time, although evidence of Palaeolithic occupation is present from Gorham's Cave at Gibraltar (e.g., Pettitt & Bailey, 2000).

The sedimentological, geochemical and microfaunal results of M2 and M3 suggest a transition from shallow marine (below approx. 8.00 m b.s.) to open lagoonal and finally closed lagoonal conditions (above ~5.50 m b.s.). <sup>14</sup>C-AMS ages from Facies C in G9, G6 and G2 as well as M2 and M3 (cf. Table 1, Figure 10) suggest that this transition occurred already during the mid-Holocene, that is, around or shortly after 6000 B.C., during the Neolithic period (~5500 B.C., Figure 13b). This may be explained by the evolution of a barrier in the seaward sections of the former embayment (e.g., at G7; Figures 10 and 11) at a time when local RSL rise decelerated (Vacchi et al., 2016) and littoral processes dominated coastal evolution. In any case, shallow marine deposits with fluctuating depositional conditions at G7 suggest that the sandy barrier and/or probably also delta-type conditions shifted seawards, resulting in open lagoonal environments in large parts of the former embayment. Sandy barrier to sublittoral deposits were also documented at G11 sometime before 4300 cal B.C.

In the lagoonal deposits (Facies C), autochthonous species (i.e., lagoonal species) coexist with allochthonous species of shallow marine origin; however, most of these allochthonous species are of pre-Holocene or even pre-Quaternary origin, which indicates an alluvial (Río Guadiaro) or even colluvial (adjacent slopes, Pliocene sedimentary rocks) sediment input. Variations in the content of these allochthonous species may be used as a proxy for either increased fluvial input and proximity of the Río Guadiaro or slope activity and erosion (i.e., colluvial sediment input): periods with river proximity and/or higher slope activity and erosion are separated by periods when lagoonal conditions with predominantly autochthonous, fine-grained sedimentation prevailed.

From around 5000 B.C., rates of local RSL rise are assumed to have further decreased in southern Spain (cf. Vacchi et al., 2016; Zazo et al., 2008). The lagoonal conditions seem to have prevailed in most of the study area during the Neolithic, but a fluvial input in the seaward cores (e.g., G11) is suggested by high sand contents in mud layers and/or sand-dominated layers dating to ca. 4300 B.C. Unfortunately, no chronological information is available in the landward cores G8 and G9 from these periods. However, the chronological information from Facies C suggests that lagoonal

conditions ceased around or before c. 2000–2500 B.C.: in all cores, <sup>14</sup>C-AMS ages from samples of Facies C are older than 2500 B.C. Instead, the ERT transects and sediment cores document several palaeo-channels of the Río Guadiaro, which had incised into the underlying lagoonal deposits and accumulated thick units of coarse (sand and gravel) deposits (Facies F; G2, G6, G8, G9, M4, M5) (Figures 2, 3 and 9). At G8, for instance, two units of fluvial deposits were separated by the temporary establishment of still-water conditions around 2700 cal B.C. (G8/12 PR), reflecting freshwater environments and highly dynamic conditions with a rather rapid shift and subsequent abandonment of river channels. At the end of the Neolithic and during the Chalcolithic period (Figure 13c), a fluvial landscape thus started to develop in the lower floodplain sections of the Río Guadiaro, related to ceasing lagoonal conditions and the successive evolution of the floodplain. Channel deposits are dated to this period in cores G8 and G6, and channel deposits in cores M4 and M5 may be related to these river courses as well. Where no river channel deposits were documented (cores G5, M2, M3), the lagoonal sediments are gradually replaced by alluvial sediments of Facies E. For the Chalcolithic settlement of El Alto, however, the lagoon may have still provided an important food source, although such evidence (e.g., eating waste such as mollusc shells or fish bones) was not found during the archaeological surface survey within the framework of Archeostraitis.

With the settlement of Montilla, human occupation is for the first time documented in the lower elevations along the evolving floodplain in the Final Bronze Age. At G6 and G2, <sup>14</sup>C-AMS ages indicate that around or after ~1800 cal B.C. (G6/12+ HR) and ~100 cal B.C. (G2/17 PR, Table 1; Figure 11), respectively, the Río Guadiaro course (Facies F) had shifted further towards the northeast. Although precise dating of the timing of related channel activity is not possible due to probable reworking effects of the dated material, the general pattern of subsurface channel deposits and the <sup>14</sup>C-AMS-based chronostratigraphy suggests that, at the transition from the Bronze Age to the Iron Age, and therefore at the time of Phoenician appearance along the Andalusian coastline, meandering of river channels or channel bifurcation led to a position of the Río Guadiaro close to Montilla (Figures 9, 11 and 13).

At that time, locations along the evolving floodplain seem to have become increasingly attractive, for example, due to the river as a transport pathway. Trading pathways were likely directed from Montilla towards Los Castillejos de Alcorrín via El Alto and *vice versa*. Managed and/or used by the local population under the rule of Los Castillejos de Alcorrín, Montilla represented a protected interface controlling the junction of the riverine with mainland (native) trade routes. Against the background of the rich metal resources in the hinterland (e.g., area of Ronda; Aguayo de Hoyos, 1997; Aguayo de Hoyos, 2018; Aguayo de Hoyos & Carrilero Milan, 1991; Marzoli et al., 2014 183f.; Renzi et al., 2014, 2016), this enabled a profitable connection to the new markets established by the Phoenicians on the coast, who are assumed to have had their mooring places further south directly at the coast or at the mouth of the Guadiaro (Figure 13).

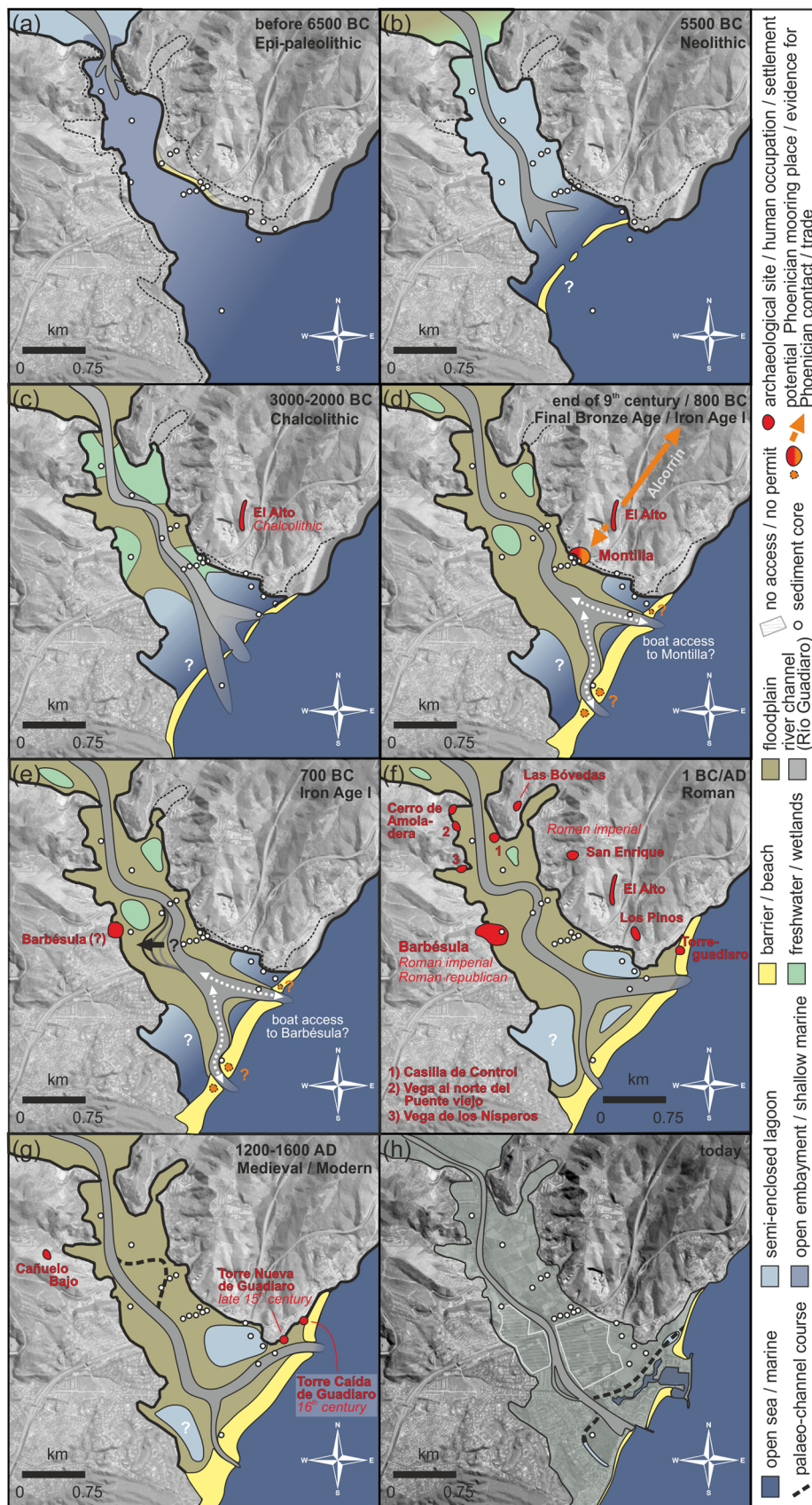


**FIGURE 13** Palaeogeographic scenarios for the study area for different archaeological periods. (a) Epi-Palaeolithic period, (b) Neolithic, (c) Chalcolithic, (d) Final Bronze Age to Iron Age I (~800 B.C.), (e) Iron Age I (~700 B.C.), (f) Roman, (g) Medieval to Modern, (h) Present. Elevation data/satellite images based on Google Earth/Maxar Technologies (2011) and freely available LiDAR data of 2 m resolution (Geoportal of the Junta de Andalucía). [Color figure can be viewed at [wileyonlinelibrary.com](https://onlinelibrary.wiley.com)]

Therefore, together with the reduced saltwater influence inferred in the upper part of the still-water deposits (Facies D), facies F and E give evidence of bifurcation and/or the shifting course of the Río Guadiaro, reflecting the development of a river-dominated landscape and the evolution of the modern floodplain. It can be assumed that the erosional base of the palaeo-channels was approximately at the same level: the base of the river-deposited coarse sediments is constantly found at ~4–5 m bsl, as the local RSL is assumed to have reached this position after 3000–4000 B.P.

Montilla was intentionally abandoned at the end of the 8th century B.C., at the same time as Los Castillejos de Alcorrín and the intervening satellite settlements (e.g., El Alto). The location as a near-coastal inland port on the Río Guadiaro may tentatively provide reasons for restructuring the settling: the river landscape was highly dynamic with a meandering river course, and the simultaneous abandonment of Montilla and the central settlement of Los Castillejos de Alcorrín may indicate such a riverine shift, through which the importance of this trade axis with the Phoenicians was lost. Similar conclusions were drawn by Rouillard et al. (2007) for the Lower Segura valley (SE Spain) in the same period, where a northward shift of the river channel in the delta area is assumed to have caused changes in the settlement pattern. **On the western side of the Guadiaro river, the settlement of Barbesula existed at least since the 6th century B.C.** There is, however, the hypothesis that it had already been settled during Iron Age I, that is, contemporaneous and/or shortly after Montilla; unfortunately, as yet, definite proof of this is missing. Whether the appearance of this settlement was related to a changing river access to Montilla (i.e., river channel shift towards the southwestern valley sections) thus remains open. However, no evidence of channel deposits was found in core B1: here, standing water bodies may have prevailed during the Iron Age times, likely related to freshwater conditions. Potential Early Iron Age to Roman river channels may be found south of core B1, an area for which work/coring permits were unfortunately not granted.

Subsequently, the Roman period is characterised by increased numbers of settlements/occupation sites in and adjacent to the floodplain. Likely, the Río Guadiaro served as a major route to access the hinterland, which was controlled by towers at the narrow valley section close to G9 (Figure 13). Terrestrial conditions must have established seawards of Torreguadiaro, where Roman remains are documented, which is somewhat in contrast to the findings from coring transect C, where littoral and subsequent lagoonal conditions were inferred for the period after A.D. 1000. However, the Roman remains may suggest that the estuary river mouth was directed towards the northeast at that time, which was likely associated with the fluvial deposits in cores G4, G11 and G12. An open or semi-enclosed lagoon can be assumed for this area, which was separated from the open sea by a sand barrier. This barrier may have served as a suitable place for human occupation, controlling the entrance to the estuary. Furthermore, the floodplain deposits directly below the thick artefact-bearing layer of Barbesula at B1 suggest a shift of the main river channel towards the western valley side shortly before or during Roman times, when the accumulation of floodplain deposits led to terrestrial conditions in this

area. However, as mentioned before, no direct evidence of channel deposits was found in B1.

Finally, the siltation of the Guadiaro alluvial plain and the shift towards terrestrial conditions in the southeast of Montilla seems to have taken place only within the past 1000 or so years. G3 (Figure 11) indicates high sedimentation rates in the most recent centuries, which could be connected, for example, to an eastward shift of the main channel of the Guadiaro estuary, as can also be assumed due to the two tower systems of modern age (late 15th and 16th centuries) located close to the village of Torreguadiaro. Although fluctuating depositional conditions at G11 (Figure 11) suggest a period of fluvio-marine deposition already around or after ~4350 cal B.C. (G11/20+ PR, 6.75 m b.s.) and thus the presence of the Río Guadiaro estuary in the seaward part of the Guadiaro valley at that time, the final evolution of the floodplain and the shift towards terrestrial conditions dates back to the last few hundred years, when remaining lagoons or swamps must have disappeared, likely supported by human drainage activities during the last centuries. The main estuary shifted to the present position, leading to the abandonment of the Roman to 16th century river mouth.

## 5.2 | Montilla during the early Phoenician colonisation

### 5.2.1 | Stratigraphical correlation with previous results

Based on the study presented here, and particularly based on the findings of transect B and the results from cores M1, M3 and M7, the sedimentary succession in the surroundings of Montilla and its palaeoenvironmental interpretation is in general agreement with the findings of Hoffmann (1988a,b) and Schubart (1988). Core M1 (e.g., Figure 9) with a ~2 m thick layer with abundant artefacts (Facies O) reflects the findings along the NW sections of coring profiles I and II in Hoffmann (1988a) (cf. Figure 12). The sterile light brown sand at the base was dated to a pre-Holocene age using OSL (minimum age of 190 ka); it may tentatively be interpreted as terrace deposits of a Pleistocene Palaeo-Guadiaro. These deposits cover the Neogene sandstone (Facies N), encountered at the very base of cores M1, M3, M7 and M9, which is characterised by an abundance of marine microfauna.

Interestingly, the <sup>14</sup>C-AMS age of charcoal remains from the thin palaeosol on top of the Pleistocene terrace deposits at M1 suggests an occupation layer/ground floor at 2.23 m b.s. during the Early Iron Age, that is, the Phoenician period (809–549 cal B.C., M1/8 HK; Facies P). This is in perfect agreement with the Phoenician pottery remains in the layers of Facies O above, dated to the 8th century B.C. (Figure 8). Apparently, both the Pleistocene terrace (in M1) and the Neogene deposits (e.g., at T2; Schubart, 1988) served as the occupation layer/ground floor during the time Montilla was used as a settlement/trading post.

The 40–50 cm thick light brown sand layer with stones in T3 Schubart (1988) is assumed to be related to the highly resistant

sediments of the interrupted cores and the whitish brown sandy horizon at ~1.20–1.40 m b.s. intercalating Facies O particularly in M7 but also in M1 and M9. This suggests the presence of a stone-enriched (occupation?) horizon of anthropogenic origin (e.g., a stone pavement) at that depth in the easternmost floodplain sections of transect C, which may have been intentionally put in place (Figure 8).

Below, Schubart (1988) described a grey layer of loam with abundant Phoenician ceramics, which covers the Neogene sandstone at ~0.5–1.0 m asl. Ceramic fragments were also found at similar depth until ~0 m asl (~2.80 m b.s.) in M7 (i.e., a position comparable to core 39 in Hoffmann, 1988a), in a silt-dominated (15–30  $\mu\text{m}$ , 5% clay) slightly greyish to brown horizon containing some well-rounded fine- to medium-sized pebbles and few stones. According to the geochemical and sedimentological analyses, and in agreement with the other cores from this study and the study of Hoffmann (1988a; his cores 39, 54), this core section of M7 may be related to the transition from a freshwater-dominated semiterrestrial environment with (temporary?) coastal lakes (below 2.50 m b.s.) to the evolving alluvial floodplain (Facies F, above 2.50 m b.s.). This suggests that flood deposits of the Río Guadiaro interfinger with the Montilla-related ceramic-containing (colluvial) deposits. This could generally be due to (i) the presence of a settlement/trading post during Phoenician times in the easternmost floodplain sections along coring transect B, affected by temporary flooding events of the Río Guadiaro; or (ii) the presence of a settlement/trading post during Phoenician times in direct vicinity to the floodplain, the remains of which were eroded and transported to the floodplain after its abandonment (colluvial origin). While this facies succession is generally similar in the upper part of M3, located a few metres further west and inside the floodplain, the ceramic-containing (colluvial and/or alluvial) layers here are rather indistinct and characterised by few small ceramic fragments, found only above 2 m b.s. This generally suggests a decreasing input of anthropogenic materials towards the floodplain. In addition, according to the PCA, the transition to floodplain sedimentation of Facies F at M3 may have occurred between ~2.80 and 2.50 m b.s., that is, before an interfingering with (colluvial) ceramic-containing deposits is documented (Figure 12).

As the upper boundary of the pre-Holocene surface at M7 is approx. 2 m lower than in the other surrounding cores M1 and M9 as well as in the excavation T3 described in Schubart (1988) (Figure 12), the palaeo-topography, related to the palaeo-surface associated with the Phoenician occupation layer/ground floor found in M1, seems to indicate a topographical low at M7, which is stretching a few metres towards the former settlement of Montilla. This situation may explain the existence of the stone layer (pavement?) in M7, which may tentatively be regarded as a countermeasure against swampy conditions, and it also explains the different sedimentary succession at M7, starting with (peat-like) Facies C directly above the Neogene Facies N.

In this area, Phoenician ceramic fragments are reported to have been found in a grey mud-dominated unit (i.e., a unit similar to Facies C in M7) reaching down to 1.50 m bsl (5.70 m b.s.), directly covering

the Neogene basement in core 39 of Hoffmann (1988a). This layer was interpreted to be of marginal marine origin by Hoffmann (1988a,b), implying that the coastline was located in direct adjacency of Montilla during the Phoenician presence (Schubart, 1988). In contrast to these studies, however, ceramic fragments were only found until ~0 bsl (~2.80 m b.s.) in the alluvial Facies F of M7: in the underlying Facies C (0–1.20 m bsl), which comprised abundant plant/root remains and a peat-like organic-rich layer at the base and which may be considered similar to the basal deposits described in core 39 of Hoffmann (1988a,b), not a single ceramic fragment was documented. According to the  $^{14}\text{C}$ -AMS dating results of root remains from this layer, these sediments accumulated sometime between ~4400 cal B.C. (~1 m bsl/3.85 m b.s.) and ~2600 cal B.C. (0.5 m bsl/3.35 m b.s.), which agrees with  $^{14}\text{C}$ -AMS ages of further cores in the surroundings (M3, ~4200 cal B.C. at ~1 m bsl) (Figure 12).

## 5.2.2 | Montilla, a river harbour for trade and exchange with the Phoenicians?

The apparent discrepancy between the findings of Hoffmann (1988a,b) and the chronostratigraphical information obtained from similar strata in this study involves some challenges regarding the palaeoenvironmental reconstructions during the Phoenician times. Assuming that (i) the dating results of the root remains obtained from M7 are not biased by the old carbon effect or reworking of dated plant material, and that (ii) the general chronostratigraphical pattern and facies succession along the lower Río Guadiaro inferred by our study is correct, the lagoonal to marginal marine deposits of M7 are too old for a Phoenician influence. This raises the question why Phoenician ceramics were found in these deposits in the previous study. In any case, the general chronostratigraphical pattern in the evolution of the lower Guadiaro floodplain, as inferred from numerous  $^{14}\text{C}$ -AMS ages of our study, suggests that marginal marine environments and the floodplain of the Río Guadiaro had already migrated seawards at the Phoenician time, resulting in the accumulation of alluvial deposits (overbank fines) in the Montilla area. Another explanation for the observed discrepancy may be found in the coring technique used in the 1980s, that is, a rotary hand auger recovering ca. 20 cm of new core material only with each single drilling operation; this may well have displaced ceramic fragments during recovery of the coring head when crossing the resistant and ceramic-rich strata at 1.20–1.40 m b.s. Finally, the discrepancy may be explained by anthropogenic dredging in the area of coring profile I of Hoffmann (1988a,b), which may have affected coring location 39 but not M7 of this study. However, these questions cannot be solved conclusively based on the data at hand.

As discussed before, lagoonal environments ceased during the 3rd millennium B.C. in the area around Montilla. In agreement with the evolution of other coastal lowlands in southern Spain (e.g., Brisset et al., 2018; May et al., 2021), delta progradation, floodplain evolution and the seaward migration of the coastline to approximately its present location had already taken place before the Phoenicians arrived in

southern Iberia, resulting in a river-dominated landscape in the lower Guadiaro valley at that time. Lagoonal conditions at Montilla had thus likely already disappeared during Phoenician times, and a direct access by boat (e.g., in the form of a lagoonal coastline) to the settlement, postulated in previous research (Hoffmann, 1988a,b; Schubart, 1988), could not be confirmed. At that time, the deposition of overbank fines related to the evolution of the alluvial plain already took place in that area, as discussed in the previous section. Since no Holocene fluvial deposits were found in the direct vicinity of Montilla (transect B, cores M1–3, 7–9), a direct connection of Montilla to the open sea via the Río Guadiaro, that is, in the form of a river harbour directly at the settlement site, must also be considered unlikely. However, our results from transect A suggest that at around or after ~1800 cal. B.C. (G6) and/or ~85 cal. B.C. (G2), the course of the Río Guadiaro had shifted to the northeast of the modern channel, that is, several hundred metres closer to the settlement of Montilla. This former course of the Río Guadiaro (Figure 9) represented a likely access to Montilla during the Final Bronze and Early Iron Age, that is, during the time of Phoenician contact, potentially related to suitable mooring locations close to Montilla. At the junction of the riverine trade routes to the hinterland offering rich metal resources (Aguayo de Hoyos & Carrilero Milan, 1991; Aguayo de Hoyos, 1997; Aguayo de Hoyos, 2018; Marzoli et al., 2014; 183f.; Renzi et al., 2016) and the mainland (native) trade routes towards Los Castillejos de Alcorrín, Montilla likely served as a profitable connection to the new markets established by the Phoenicians on the coast.

## 6 | CONCLUSIONS

Based on sedimentological, geochemical, chronological and micro-faunal analyses of 22 vibracores from the lower Río Guadiaro (Málaga, Andalusia), this geoarchaeological study reconstructed mid- to late Holocene environments and coastal changes in the context of the Early Iron Age settlement of Montilla, which has been considered an indigenous to Phoenician harbour site of Los Castillejos de Alcorrín based on previous investigations.

Our interpretation of ERT- and coring transects carried out in the floodplain of the lower Río Guadiaro allows for the differentiation of successive palaeoenvironments and for establishing a local chrono-stratigraphy for the sedimentary infill of the valley. Based on these results, the deposition of shallow marine sands and overlying deltaic deposits of alternating sand and mud took place before ~5500 B.C., followed by a long period of lagoonal conditions until ~2500 B.C. Around that time, lagoonal conditions ceased and a fluvial landscape developed, characterised by shifting river channels, standing water bodies with freshwater conditions and the evolution of the modern floodplain by alluvial sedimentation.

In contrast to the previous investigations, our results suggest that the Phoenicians encountered a river-dominated landscape when establishing first trading contacts in Andalusia in the 8th century B.C. Access to Montilla by boat was most likely via an old branch of the Río Guadiaro, which was, although not providing direct access to the site, located closer to Montilla than the present channel. Subsequent

channel shifts/dynamics likely resulted in the abandonment of the site before 700 B.C., and the (assumed) appearance of Barbesula on the opposite (SW) side of the valley during the 7th century B.C. may point to a river channel shift towards the SW valley sections.

Finally, it may tentatively be assumed that these palaeoenvironmental changes had considerable influence on local occupation patterns. One of the reasons, if not the most important one, for the rather rapid (and non-destructive) abandonment of Los Castillejos de Alcorrín and its related settlements including Montilla may be seen in the dynamics of the estuary channels. More explicitly, the contemporaneous/simultaneous abandonment of Montilla and Alcorrín after the 8th century B.C. may be explained with a shift of the river channel towards the SW Río Guadiaro valley section, which may have resulted in a decreasing importance of the trading pathways along this trajectory.

## ACKNOWLEDGEMENTS

This study was carried out within the framework of the German-French interdisciplinary project 'Archeostraits', funded by the DFG (MA 1774/2-1) and the ANR (ANR-13-FRAL-0011-01). The project was led by Prof. Dr. Dirce Marzoli (DAI Madrid; Mediterranean part) and Prof. Dr. Pierre Moret (Université Toulouse II; Atlantic part). Geoarchaeological investigations were carried out under supervision of Prof. Dr. Helmut Brückner (University of Cologne). Jule Rump, Daniel Blum (Cologne), Gilles Rixhon (Strasbourg) and Melanie Bartz (Lausanne) helped during field work and laboratory analyses. The Junta de Andalucía kindly granted the research permits for both the archaeological survey and the geoarchaeological investigations. Open Access funding enabled and organized by Projekt DEAL.

## CONFLICT OF INTEREST

The authors declare no conflict of interest.

## ORCID

Simon Matthias May  <http://orcid.org/0000-0001-6762-7500>

Helmut Brückner  <http://orcid.org/0000-0002-2130-5394>

## REFERENCES

- Aguayo de Hoyos, P. (1997). Análisis territorial de la ocupación humana en la depresión de Ronda durante la prehistoria reciente. In J. M. Martín Ruiz, & P. J. Sánchez Bandera (Eds.), *Arqueología a la Carta. Relaciones entre teoría y método en la práctica arqueológica* (pp. 9–34).
- Aguayo de Hoyos, P. (2018). La problemática de la transmisión tecnológica: el caso de la metalurgia protohistórica en el extremo Occidente mediterráneo. Implicaciones desde el registro arqueológico de algunos asentamientos del interior de los sistemas béticos (Andalucía, España). In M. Guirguis (Ed.), *From the Mediterranean to the Atlantic: People, Goods and Ideas between East and West, 8th International Congress of Phoenician and Punic Studies, Carbonia, Sant'Antioco, 21th-16th October 2013, Folia Phoenicia* (pp. 231–235). Fabricio Serra Editore.
- Aguayo de Hoyos, P., & Carrilero Milan, M. (1991). La presencia fenicia y el proceso de aculturación de las comunidades del Bronce Final de la depresión de Ronda (Málaga). In Consiglio Nazionale delle Ricerche (Ed.), *Atti del II Congresso Internazionale di Studi Fenici e Punici* (pp. 559–571).



- Anthony, E. J., Marriner, N., & Morhange, C. (2014). Human influence and the changing geomorphology of Mediterranean deltas and coasts over the last 6000 years: From progradation to destruction phase? *Earth-Science Reviews*, 139, 336–361. <https://doi.org/10.1016/j.earscirev.2014.10.003>
- Armstrong, H. A., & Brasier, M. D. (2005). *Microfossils*. Blackwell Publishing.
- Arteaga, O., Kölling, A., Kölling, M., Roos, A. M., Schulz, H., & Schulz, H. D. (2004). Geschichte des Küstenverlaufs im Stadtgebiet von Cádiz. *Madrider Mitteilungen*, 45, 181–215.
- Arteaga, O., Schulz, H. D., & Roos, A. M. (2008). Geoarqueología dialéctica en la Bahía de Cádiz. *Revista Atlántica-Mediterránea de Prehistoria y Arqueología Social*, 10, 21–116.
- Aubet, M. E. (2006). *The Phoenicians and the west: Politics, colonies and trade* (2nd ed.). Cambridge University Press.
- Aubet, M. E. (2009). *Tiro y las colonias fenicias de Occidente*. Edicions Bellaterra.
- Aubet, M. E. (2016). Phoenicians abroad: From merchant venturers to colonists. In M. Fernández-Götz & D. Krausse (Eds.), *Eurasia at the dawn of history. Urbanization and Social Change* (pp. 254–264).
- Bellin, N., Vanacker, V., & De Baets, S. (2013). Anthropogenic and climatic impact on holocene sediment dynamics in SE Spain: A review. *Quaternary International*, 308–309, 112–129. <https://doi.org/10.1016/j.quaint.2013.03.015>
- Blott, S. J., & Pye, K. (2001). GRADISTAT: A grain size distribution and statistics package for the analysis of unconsolidated sediments. *Earth Surface Processes and Landforms*, 26, 1237–1248. <https://doi.org/10.1002/esp.261>
- Brisset, E., Burjachs, F., Ballesteros Navarro, B. J., & Fernández-López de Pablo, J. (2018). Socio-ecological adaptation to Early-Holocene sea-level rise in the western Mediterranean. *Global and Planetary Change*, 169, 156–167.
- Carrión, J. S., Fernández, S., Jiménez-Moreno, G., Fauquette, S., Gil-Romera, G., González-Sampériz, P., & Finlayson, C. (2010). The historical origins of aridity and vegetation degradation in southeastern Spain. *Journal of Arid Environments*, 74, 731–736. <https://doi.org/10.1016/j.jaridenv.2008.11.014>
- Castro, P. V., Chapman, R. W., Gili, S., Lull, V., Micó, R., Rihuete, C., Risch, R., & Sanahuja Yll, E., (1998). *Aguas Project. Palaeoclimatic reconstruction and the dynamics of human settlement and land use in the area of the Middle Aguas (Almería), in the south-east of the Iberian Peninsula*. European Commission Environment and Climate Programme, Final report on Contract EV5V-CT94-0487.
- Cearreta, A., Benito, X., Ibáñez, C., Trobajo, R., & Giosan, L. (2016). Holocene palaeoenvironmental evolution of the Ebro Delta (Western Mediterranean Sea): Evidence for an early construction based on the benthic foraminiferal record. *The Holocene*, 26(9), 1438–1456.
- Cimerman, F., & Langer, M. R. (1991). Mediterranean foraminifera. *Slovenska Akademija Znanosti in Umetnosti* 30, 118.
- Corella, J. P., Moreno, A., Morellón, M., Rull, V., Giral, S., Rico, M. T., Pérez-Sanz, A. & Valero-Garcés, B. L. (2011). Climate and human impact on a meromictic lake during the last 6,000 years (Montcortès Lake, Central Pyrenees, Spain). *Journal of Paleolimnology*, 46, 351–367. <https://doi.org/10.1007/s10933-010-9443-3>
- Dabrio, C. J., Zazo, C., Goy, J. L., Sierro, F. J., Borja, F., Lario, J., González, J. A., & Flores, J. A. (2000). Depositional history of estuarine infill during the last postglacial transgression (Gulf of Cadiz, southern Spain). *Marine Geology*, 162, 381–404. [https://doi.org/10.1016/S0025-3227\(99\)00069-9](https://doi.org/10.1016/S0025-3227(99)00069-9)
- Durcan, J. A., King, G. E., & Duller, G. A. T. (2015). DRAC: Dose Rate and Age Calculator for trapped charge dating. *Quaternary Geochronology*, 28, 54–61.
- Fernández-Salas, L., Lobo, F. J., Hernández-Molina, F. J., Somoza, L., Rodero, J., del Río, V. D., & Maldonado, A. (2003). High-resolution architecture of late Holocene highstand prodeltaic deposits from southern Spain: The imprint of high-frequency climatic and relative sea-level changes. *Continental Shelf Research*, 23(11–13), 1037–1054.
- Folk, R. L., & Ward, W. C. (1957). Brazos River bar [Texas]: A study in the significance of grain size parameters. *Journal of Sedimentary Research*, 27, 3–26. <https://doi.org/10.1306/74D70646-2B21-11D7-8648000102C1865D>
- Galbraith, R. F., Roberts, R. G., Laslett, G. M., Yoshida, H., & Olley, J. M. (1999). Optical dating of single and multiple grains of quartz from Jinmium rock shelter, northern Australia: Part I, Experimental design and statistical models. *Archaeometry*, 41, 339–364.
- García-Artola, A., Stéphan, P., Cearreta, A., Kopp, R. E., Khan, N. S., & Horton, B. P. (2018). Holocene sea-level database from the Atlantic coast of Europe. *Quaternary Science Reviews*, 196, 177–192. <https://doi.org/10.1016/j.quascirev.2018.07.031>
- Gibbons, W., & Moreno, T. (Eds.). (2002). *The geology of Spain*. Geological Society of London.
- González-Castillo, L., Galindo-Zaldívar, J., Junge, A., Martínez-Moreno, F. J., Löwer, A., Sanz de Galdeano, C., Pedrera, A., López-Garrido, A. C., Ruiz-Constán, A., Ruano, P., & Martínez-Martos, M. (2015). Evidence of a large deep conductive body within the basement of the Guadalquivir foreland Basin (Betic Cordillera, S-Spain) from tipper vector modelling: Tectonic implications. *Tectonophysics*, 663, 354–363. <https://doi.org/10.1016/j.tecto.2015.08.013>
- Goy, J. L., Zazo, C., & Dabrio, C. J. (2003). A beach-ridge progradation complex reflecting periodical sea-level and climate variability during the Holocene (Gulf of Almería, Western Mediterranean). *Geomorphology*, 50(1–3), 251–268.
- Grützner, C., Reicherter, K., Hübscher, C., & Silva, P. G. (2012). Active faulting and neotectonics in the Baelo Claudia area, Campo de Gibraltar (southern Spain). *Tectonophysics*, 554–557, 127–142. <https://doi.org/10.1016/j.tecto.2012.05.025>
- Gutierrez de Ravae Aguera, E., Peinado, A., Giraldez Cervera, J. V., Ayuso Muñoz, J. L. (1986). La distribución de la lluvia en Andalucía. *El Agua en Andalucía* 2, 23–35.
- Gutiérrez López, J. M., Reinoso del Río, M. C., Saez Romero, A. M., Giles Pacheco, F., Finlayson, J. C., & Zamora Lopez, J. A. (2014). El Santuario de la Cueva de Gorham (Gibraltar). In A. Lemaire (Ed.), *Phéniciens d'Orient et de l'Occident* (pp. 619–629). Editions Jean Maisonneuve.
- Hammer, Ø., Harper, D. A., & Ryan, P. D. (2001). PAST: Paleontological statistics software package for education and data analysis. *Palaeontologia Electronica*, 4(1), 9.
- Heaton, T. J., Köhler, P., Butzin, M., Bard, E., Reimer, R. W., Austin, W. E. N., Bronk Ramsey, C., Grootes, P. M., Hughen, K. A., Kromer, B., Reimer, P. J., Adkins, J., Burke, A., Cook, M. S., Olsen, J., Skinner, L. C. (2020). Marine20—The marine radiocarbon age calibration curve (0–55,000 cal BP). *Radiocarbon*, 62(4), 779–820. <https://doi.org/10.1017/RDC.2020.68>
- Hoffmann, G. (1988a). Geologische Untersuchungen im Tal des Río Guadiaro, Prov. Cádiz. *Madrider Mitteilungen* 29, 126–131.
- Hoffmann, G. (1988b). *Holozänstratigraphie und Küstenlinienvorlagerung an der andalusischen Mittelmeerküste* (p. 180). Bremen (Berichte aus dem Fachbereich Geowissenschaften der Universität Bremen, 2).
- Jalut, G., Dedoubat, J. J., Fontugne, M., & Otto, T. (2009). Holocene circum-Mediterranean vegetation changes: Climate forcing and human impact. *Quaternary International*, 200, 4–18. <https://doi.org/10.1016/j.quaint.2008.03.012>
- Joachim, F., & Langer, M. R. (2008). *The 80 most common ostracods from the Bay of Fetoveia, Elba Island (Mediterranean Sea)*. Selbstverlag Universität Bonn.
- Karanovic, I. (2012). *Recent freshwater ostracods of the world. Crustacea, ostracoda, podocopida*. Springer.
- Köppen, W. P., & Geiger, R. (1968). *Klima der Erde: Climate of the Earth*. Perthes.
- Lambeck, K., Yokoyama, Y., & Purcell, T. (2002). Into and out of the Last Glacial Maximum: Sea-level change during Oxygen Isotope Stages 3

- and 2. *Quaternary Science Reviews*, 21, 343–360. [https://doi.org/10.1016/S0277-3791\(01\)00071-3](https://doi.org/10.1016/S0277-3791(01)00071-3)
- Lario, J., Zazo, C., Goy, J. L., Dabrio, C. J., Borja, F., Silva, P. G., Sierro, F., González, A., Soler, V., & Yll, E. (2002). Changes in sedimentation trends in SW Iberia Holocene estuaries (Spain). *Quaternary International*, 93–94, 171–176. [https://doi.org/10.1016/S1040-6182\(02\)00015-0](https://doi.org/10.1016/S1040-6182(02)00015-0)
- López Sáez, J. A., García, P. L., & Sánchez, M. (2002). Palaeoecology and Holocene environmental change from a saline lake in South-West Spain: Protohistorical and prehistorical vegetation in Cádiz Bay. *Quaternary International*, 93–94, 197–206. [https://doi.org/10.1016/S1040-6182\(02\)00018-6](https://doi.org/10.1016/S1040-6182(02)00018-6)
- Luterbacher, J., Xoplaki, E., Casty, C., Wanner, H., Pauling, A., Küttel, M., Rutishauser, T., Brönnimann, S., Fischer, E., Fleitmann, D., González-Rouco, F. J., García-Herrera, R., Barriendos, M., Rodrigo, F., González-Hidalgo, J. C., Saz, M. A., Gimeno, L., Ribera, P., Brunet, M., ... Ladurie, E. L. R. (2006). Mediterranean climate variability over the last centuries: a review. *Developments in Earth and Environmental Sciences*, 4, 27–148. [https://doi.org/10.1016/S1571-9197\(06\)80004-2](https://doi.org/10.1016/S1571-9197(06)80004-2)
- Martín-Chivelet, J., Berástegui, X., Rosales, I., Vilas, L., Vera, J., Caus, E., Gräfe, K.-U., Mas, R., Puig, C., Segura, M., Robles, S., Floquet, M., Quesada, S., Ruiz-Ortiz, P. A., Fregenal-Martínez, M. A., Salas, R., Arias, C., García, A., Martín-Algarra, A., ... Ortega, F. (2002). Cretaceous. In W. Gibbons & T. Moreno (Eds.), *The geology of Spain* (pp. 255–292). Geological Society of London.
- Martín-Puertas, C., Valero-Garcés, B. L., Brauer, A., Mata, M. P., Delgado-Huertas, A., & Dulski, P. (2009). The Iberian–Roman Humid Period (2600–1600 cal yr BP) in the Zoñar Lake varve record (Andalucía, southern Spain). *Quaternary Research*, 71, 108–120. <https://doi.org/10.1016/j.yqres.2008.10.004>
- Marzoli, D. (2012). Neugründungen im phönizischen Westen. Los Castillejos de Alcorrín, Morro de Mezquitilla und Mogador. *Archäologischer Anzeiger*, 2012(2), 29–64. <https://publications.dainst.org/journals/aa/121/4806>
- Marzoli, D. (2015). Die Phönizier auf der Iberischen Halbinsel. In A.-M. Wittke (Eds.), *Frühgeschichte der Mittelmeerkulturen. Historisch-archäologisches Handbuch, Der Neue Pauly* (Suppl. Bd. 10, 2.1.12, pp. 179–188). J. B. Metzlersche Verlagsbuchhandlung and Carl Ernst Poeschel Verlag GmbH.
- Marzoli, D. (2018). Rencontres entre Orient et Occident: les Phéniciens le long des côtes de la péninsule Ibérique et du Maroc. *Dialogues d'histoire ancienne*, 44/1, 225–251.
- Marzoli, D. (2020). Phönizische und einheimische Akteure früher Ost-West-Begegnungen am Rand der alten Welt (Ende 9. bis 7. Jahrhundert v. Chr.). In D. Marzoli, S. Reinhold, U. Schlotzhauer, & B. Vogt (Eds.), *Kontaktmodi. Ergebnisse der gemeinsamen Treffen der Arbeitsgruppen Mobilität und Migration und "Zonen der Interaktion" (2013–2018) ForschungsCluster 6 "Connecting Cultures"* (pp. 157–202). Formen, Wege und Räume kultureller Interaktion 2, Menschen–Kulturen–Traditionen 17 (Wiesbaden 2020).
- Marzoli, D., González-Wagner, C., Suárez-Padilla, J., López-Pardo, F., León-Martín, C., Thiemeyer, H., Torres-Ortiz, M. (2010). Los inicios del urbanismo en las sociedades autóctonas localizadas en el entorno del Estrecho de Gibraltar: investigaciones en Los Castillejos de Alcorrín y su territorio (Manilva, Málaga). *Menga: Revista de prehistoria de Andalucía*, 1, 153–183.
- Marzoli, D., González-Wagner, C., Suárez-Padilla, J., Mielke, D.P., López-Pardo, F., León-Martín, C., Thiemeyer, H., & Torres-Ortiz, M. (2009). Vorbericht zu den deutsch-spanischen Ausgrabungen in der endbronzezeitlichen Siedlung von Los Castillejos de Alcorrín, Manilva (Prov. Málaga) 2006 und 2007. *Madrider Mitteilungen*, 50, 118–148.
- Marzoli, D., Reinhold, S., Schlotzhauer, U., Vogt, B. (2020d). Kontaktmodi, Ergebnisse der gemeinsamen Treffen der Arbeitsgruppen "Mobilität und Migration" und "Zonen der Interaktion" (2013–2018) ForschungsCluster 6 "Connecting Cultures". Formen, Wege und Räume kultureller Interaktion. In D. Marzoli, U. Schlotzhauer, & D. Wigg-Wolf (Eds.), *"Connecting Cultures". Formen, Wege und Räume kultureller Interaktion 2, Menschen–Kulturen–Traditionen 17* (Wiesbaden 2020).
- Marzoli, D., Suárez Padilla, J., León Martín, C. (2020a). Los Castillejos de Alcorrín (Manilva, Málaga): la envergadura de una empresa autóctona en la esfera de la colonización fenicia en las proximidades del Estrecho de Gibraltar. In S. Celestino Pérez & E. Rodríguez González (Eds.), *A Journey between East and West in the Mediterranean, IX International Congress of Phoenician and Punic Studies I (Mérida 2020)* (pp. 1591–1603).
- Marzoli, D., Suárez Padilla, J., León Martín, C. (2020b). Los Castillejos de Alcorrín Manilva, Málaga: transformaciones locales e impacto colonial fenicio en el entorno del Estrecho de Gibraltar (siglos IX–VII a. C.). In A. Carretero (Ed.), *Actualidad de la investigación arqueológica en España I (2018–2019). Conferencias impartidas en el Museo Arqueológico Nacional (Madrid 2000)* (pp. 323–345). Ministerio de Cultura y Deporte.
- Marzoli, D., Suárez Padilla, J., Torres Ortiz, M., León Martín, C., Renzi, M., Tomassetti Guerra, J. M., Pérez Ramos, L., Torres Abril, F. (2020c). Los Castillejos de Alcorrín (Manilva, Málaga): un asentamiento fortificado autóctono en el contexto de la primera fase de la presencia fenicia e el entorno del Estrecho de Gibraltar (siglos IX–VIII a.C.). In J. L. López Castro (Ed.), *Entre Utica y Gadir* (pp. 269–292). Editorial Comares.
- Marzoli, D., Suárez Padilla, J., & Torres Ortiz, M. (2014). Die Meerenge von Gibraltar am Übergang von der Bronze- zur Eisenzeit (9.–8. Jh. v. Chr.: Zum Forschungsstand. *Madrider Mitteilungen*, 55, 167–211.
- May, S. M., Norpoth, M., Pint, A., Shumilovskikh, L., Raith, K., Brill, D., Rixhon, G., Moret, P., Jiménez-Vialás, H., Grau-Mira, I., García-Jiménez, I., Marzoli, D., León-Martín, C., Reicherter, K., Brückner, H. (2021). Mid- to late Holocene environmental changes and human-environment interactions in the surroundings of La Silla del Papa, SW Spain. *Ge archaeology*, 36(4), 573–600. <https://doi.org/10.1002/geo.21846>
- Meisch, C. (2000). *Süßwasserfauna von Mitteleuropa*. Spektrum Akademischer Verlag.
- Milker, Y. & Schmiel, G. (2012). A taxonomic guide to modern benthic shelf foraminifera of the Western Mediterranean Sea. *Palaeontologia Electronica*, 15 (2), 16A, 1–134. <https://doi.org/10.26879/271>
- Moreno, A., Pérez, A., Frigola, J., Nieto-Moreno, V., Rodrigo-Gámiz, M., Martrat, B., González-Sampériz, P., Morellón, M., Martín-Puertas, C., Corella, J. P., Belmonte, Á., Sancho, C., Cacho, I., Herrera, G., Canals, M., Grimalt, J. O., Jiménez-Espejo, F., Martínez-Ruiz, F., Vegas-Vilarrúbia, T., & Valero-Garcés, B. L. (2012). The Medieval Climate Anomaly in the Iberian Peninsula reconstructed from marine and lake records. *Quaternary Science Reviews*, 43, 16–32. <https://doi.org/10.1016/j.quascirev.2012.04.007>
- Moret P., Muñoz-Vicente Á., García-Jiménez, I., Callegarin, L., Michel, O., Fabre, J.-M., Prados-Martínez, F., & Rico, C. (2008). La Silla del Papa (Tarifa, Cádiz): aux origines de Baelo Claudia. *Mélanges de la Casa de Velázquez. Nouvelle série*, 38(1), 353–367.
- Moret, P., Prados-Martínez, F., Fabre, J. M., Fernández-Rodríguez, E., García-Fernández, F. J., González, F., & Jiménez-Vialás, H. J. (2017). La Silla del Papa: hábitat y necrópolis. Campañas 2014–2016. *Mélanges de la Casa de Velázquez. Nouvelle série*, 47(1), 49–71.
- Murray, A. S., & Wintle, A. G. (2003). The single aliquot regenerative dose protocol: Potential for improvements in reliability. *Radiation Measurements*, 37, 377–381.
- Murray, J. W. (2006). *Ecology and applications of benthic foraminifera*. Cambridge University Press.
- Pappa, E. (2013). *Early Iron Ages Exchange in the West: Phoenicians in the Mediterranean and the Atlantic*. Near Eastern Studies Suppl. 43.

- Petit-Maire, N. (1990). Natural aridification or man-made desertification? A question for the future. In R. Paepke, R. W. Fairbridge, & S. Jelgersma (Eds.), *Greenhouse effect, sea level and drought* (pp. 281–285). Springer.
- Pettitt, P. B., & Bailey, R. M. (2000). AMS radiocarbon and luminescence dating of Gorham's and Vanguard Caves, Gibraltar, and implications for the Middle to Upper Palaeolithic transition in Iberia. In C. B. Stringer, R. N. E. Barton, & C. Finlayson (Eds.), *Neanderthals on the edge* (pp. 155–162). Oxbow Books.
- Pint, A., Frenzel, P., Fuhrmann, R., Scharf, B. & Wennrich, V. (2012). Distribution of *Cyprideis torosa* (Ostracoda) in Quaternary athalassic sediments in Germany and its application for palaeoecological reconstructions. *International Review of Hydrobiology*, 97(4), 330–355.
- Pint, A., Seeliger, M., Frenzel, P., Feuser, S., Erkul, E., Berndt, C., Klein, C., Pirson, F., & Brückner, H. (2015). The environs of Elaiá's ancient open harbour—A reconstruction based on microfaunal evidence. *Journal of Archaeological Science*, 54, 340–355.
- Reicherter, K. R., & Peters, G. (2005). Neotectonic evolution of the central Betic Cordilleras (southern Spain). *Tectonophysics*, 405(1–4), 191–212.
- Reimer, P. J., Austin, W. E. N., Bard, E., Bayliss, A., Blackwell, P. G., Bronk Ramsey, C., Butzin, M., Cheng H., Edwards R. L., Friedrich M., Grootes P. M., Guilderson T. P., Hajdas I., Heaton T. J., Hogg A. G., Hughen K. A., Kromer B., Manning S. W., Muscheler R., ... Talamo S. (2020). The IntCal20 Northern Hemisphere Radiocarbon Age Calibration Curve (0–55 cal kBP). *Radiocarbon*, 62(4), 725–757. <https://doi.org/10.1017/RDC.2020.41>
- Renzi, M., Bode, M., & Marzoli, D. (2016). Ausbeutung von Bergbauressourcen im Umland von Los Castillejos de Alcorrín (Manilva, Málaga) (Ende 9. und 8. Jh. v. Chr.). Ein Vorbericht. *Madridrer Mitteilungen*, 57, 139–211.
- Renzi, M., Marzoli, D., Suárez-Padilla, J., & Bode, M. (2014). Estudio analítico de los materiales arqueometalúrgicos procedentes de Los Castillejos de Alcorrín (Manilva, Málaga), yacimiento del Bronce Final/Inicios de la Edad del Hierro en el entorno del Estrecho de Gibraltar. *Madridrer Mitteilungen*, 55, 121–166.
- Roberts, N. (1990). Human-induced landscape change in south and southwest Turkey during the later Holocene. In S. Bottema, G. Entjes-Nieborg, & W. van Zeist (Eds.), *Man's Role in the Shaping of the Eastern Mediterranean Landscape* (pp. 53–67). Balkema.
- Roberts, N., Stevenson, T., Davis, B., Cheddadi, R., Brewster, S., & Rosen, A. (2004). Holocene climate, environment and cultural change in the circum-Mediterranean region. In R. W. Battarbee, F. Gasse, & C. E. Stickley (Eds.), *Past climate variability through Europe and Africa* (pp. 343–362). Springer.
- Rouillard, P., Gailledrat, É., & Sellés, F. S. (2007). *L'établissement protohistorique de La Fonteta (fin VIIIe-fin VIe siècle av. J.-C.)*. *Collection de la Casa de Velázquez*, 96. Casa de Velázquez.
- Schirmacher, J., Kneisel, J., Knitter, D., Hamer, W., Hinz, M., Schneider, R. R., & Weinelt, M. (2020). Spatial patterns of temperature, precipitation, and settlement dynamics on the Iberian Peninsula during the Chalcolithic and the Bronze Age. *Quaternary Science Reviews*, 233, 106220.
- Schröder, T., van't Hoff, J., López-Sáez, J. A., Viehberg, F., Melles, M., & Reicherter, K. (2018). Holocene climatic and environmental evolution on the southwestern Iberian Peninsula: A high-resolution multi-proxy study from Lake Medina (Cádiz, SW Spain). *Quaternary Science Reviews*, 198, 208–225. <https://doi.org/10.1016/j.quascirev.2018.08.030>
- Schubart, H. (1986). Hallazgos fenicios y del Bronce Final en la desembocadura del río Guadiaro. *Anuario Arqueológico de Andalucía*, 1986(2), 200–207
- Schubart, H. (1988). Endbronzezeitliche und phönizische Siedlungsfunde von der Guadiaro-Mündung, Prov. Cádiz. Probegrabung 1986. *Madridrer Mitteilungen*, 29, 132–173.
- Siani, G., Paterne, M., Arnold, M., Bard, E., Métivier, B., Tisnerat, N., & Bassinot, F. (2000). Radiocarbon reservoir ages in the Mediterranean Sea and Black Sea. *Radiocarbon*, 42, 271–280.
- Suárez Padilla, J., Marzoli, D. (2013). La primera presencia fenicia y su relación con las comunidades indígenas a las puertas del Estrecho de Gibraltar. Investigaciones en Los Castillejos de Alcorrín (Manilva, Málaga) y la Plaza de la Catedral (Ceuta) In Instituto de Estudios Ceuties (Ed.), *Arqueología en la Columnas de Hércules. Novedades y nuevas perspectivas de la investigación arqueológica en el Estrecho de Gibraltar. XV Jornadas de Historia de Ceuta 25–28 de septiembre de 2012* (pp. 171–193).
- Van Andel, T. H., & Zangger, E. (1990). Landscape stability and destabilisation in the prehistory of Greece. In S. Bottema, G. Entjes-Nieborg, & W. Van Zeist (Eds.), *Man's role in the shaping of the Eastern Mediterranean landscape* (pp. 139–157). Balkema.
- Vacchi, M., Marriner, N., Morhange, C., Spada, G., Fontana, A., & Rovere, A. (2016). Multiproxy assessment of Holocene relative sea-level changes in the western Mediterranean: Sea-level variability and improvements in the definition of the isostatic signal. *Earth-Science Reviews*, 155, 172–197. <https://doi.org/10.1016/j.earscirev.2016.02.002>
- Vergés, J., & Fernández, M. (2012). Tethys–Atlantic interaction along the Iberia–Africa plate boundary: The Betic–Rif orogenic system. *Tectonophysics*, 579, 144–172. <https://doi.org/10.1016/j.tecto.2012.08.032>
- Wainwright, J. (1994). Anthropogenic factors in the degradation of semi-arid regions: a prehistoric case study in Southern France. In A. C. Millington, & K. Pye (Eds.), *Effects of environmental change on drylands* (pp. 285–304). John Wiley and Sons.
- Wolf, D., & Faust, D. (2015). Western Mediterranean environmental changes: Evidence from fluvial archives. *Quaternary Science Reviews*, 122, 30–50. <https://doi.org/10.1016/j.quascirev.2015.04.016>
- Zanchetta, G., Drysdale, R. N., Hellstrom, J. C., Fallick, A. E., Isola, I., Gagan, M. K., & Pareschi, M. T. (2007). Enhanced rainfall in the Western Mediterranean during deposition of sapropel S1: Stalagmite evidence from Corchia cave (Central Italy). *Quaternary Science Reviews*, 26(3–4), 279–286.
- Zazo, C., Dabrio, C. J., Goy, J. L., Lario, J., Cabero, A., Silva, P. G., Bardají, T., Mercier, N., Borja, F., & Roquero, E. (2008). The coastal archives of the last 15ka in the Atlantic–Mediterranean Spanish linkage area: Sea level and climate changes. *Quaternary International*, 181, 72–87.
- Zazo, C., Goy, J. L., Somoza, L., Dabrio, C. J., Belluomini, G., Improta, S., Lario, J., Bardají, T., & Silva, P. G. (1994). Holocene sequence of sea-level fluctuations in relation to climatic trends in the Atlantic-Mediterranean linkage coast. *Journal of Coastal Research*, 10(4), 933–945.
- Zazo, C., Silva, P. G., Goy, J. L., Hillaire-Marcel, C., Ghaleb, B., Lario, J., Bardají, T., & González, A. (1999). Coastal uplift in continental collision plate boundaries: Data from the Last Interglacial marine terraces of the Gibraltar Strait area (south Spain). *Tectonophysics*, 301, 95–109. [https://doi.org/10.1016/S0040-1951\(98\)00217-0](https://doi.org/10.1016/S0040-1951(98)00217-0)

## SUPPORTING INFORMATION

Additional supporting information can be found online in the Supporting Information section at the end of this article.

**How to cite this article:** May, S. M., Brückner, H., Norpoth, M., Pint, A., Wolf, D., Brill, D., Martín, C. L., Stika, H.-P., Padilla, J. S., Moret, P., & Marzoli, D. (2022). Holocene coastal evolution and environmental changes in the lower Río Guadiaro valley, with particular focus on the Bronze to Iron Age harbour 'Montilla' of Los Castillejos de Alcorrín (Málaga, Andalusia, Spain). *Geoarchaeology*, 1–27. <https://doi.org/10.1002/gea.21943>